

Article

Investigating the Morphometry and Hydrometeorological Variability of a Fragile Tropical Karstic Lake of the Yucatán Peninsula: Bacalar Lagoon

Laura Carrillo ^{1,*}, Mario Yescas ¹, Mario Oscar Nieto-Oropeza ¹, Manuel Elías-Gutiérrez ²,
Juan C. Alcérreca-Huerta ³, Emilio Palacios-Hernández ⁴ and Oscar F. Reyes-Mendoza ³

¹ Department of Observation and Study of the Land, the Atmosphere and the Ocean, El Colegio de la Frontera Sur (ECOSUR), Chetumal 77014, Mexico; myescas@hotmail.com (M.Y.); nietoropeza@gmail.com (M.O.N.-O.)

² Department of Systematic and Aquatic Ecology, El Colegio de la Frontera Sur (ECOSUR), Chetumal 77014, Mexico; melias@ecosur.mx

³ Department of Observation and Study of the Land, the Atmosphere and the Ocean, Ciencias y Tecnologías-El Colegio de la Frontera Sur (CONAHCYT-ECOSUR), Consejo Nacional de Humanidades, Chetumal 77014, Mexico; jalcerrech@ecosur.mx (J.C.A.-H.); oscar.reyes@ecosur.mx (O.F.R.-M.)

⁴ Department of Physics, Universidad de Guadalajara, Guadalajara 44100, Mexico; emilio.palacios@academicos.udg.mx

* Correspondence: lcarrillo@ecosur.mx



Citation: Carrillo, L.; Yescas, M.; Nieto-Oropeza, M.O.; Elías-Gutiérrez, M.; Alcérreca-Huerta, J.C.; Palacios-Hernández, E.; Reyes-Mendoza, O.F. Investigating the Morphometry and Hydrometeorological Variability of a Fragile Tropical Karstic Lake of the Yucatán Peninsula: Bacalar Lagoon. *Hydrology* **2024**, *11*, 68. <https://doi.org/10.3390/hydrology11050068>

Academic Editors: Xiaoyong Bai, Yongjun Jiang, Jian Ni, Xubo Gao, Yuemin Yue, Jiangbo Gao, Junbing Pu, Hu Ding, Qiong Xiao and Zhicai Zhang

Received: 27 March 2024

Revised: 1 May 2024

Accepted: 9 May 2024

Published: 11 May 2024



Copyright: © 2024 by the authors. Licensee MDPI, Basel, Switzerland. This article is an open access article distributed under the terms and conditions of the Creative Commons Attribution (CC BY) license (<https://creativecommons.org/licenses/by/4.0/>).

Abstract: Comprehensive morphometric and hydrometeorological studies on Bacalar Lagoon, Mexico's largest tropical karstic lake and a significant aquatic system of the Yucatán Peninsula, are lacking. This study provides a detailed analysis of its bathymetry, morphometry, and hydrometeorological characteristics. The lake's main basin stretches more than 52.7 km in length, with widths varying from 0.18 km to 2.28 km. It has a volume of 554.4 million cubic meters, with an average depth of 8.85 m, reaching depths of up to 26 m in the north and featuring sub-lacustrine dolines in the south, with depths of 38 m, 48.5 m, and 63.6 m. The study reveals seasonal variations in surface water temperature, closely linked to air temperature ($r = 0.89$), and immediate responses of water levels to hydrometeorological events. Water level fluctuations also exhibit seasonal patterns that are correlated with regional aquifer conditions, with a lag of 2 months after seasonal rainfall. Interannual variability in rainfall and water levels was observed. From 2010 to 2012, rainfall consistently remained below its mean climatic value, due to a prolonged La Niña event, while the exceptionally wet conditions in 2020 were also associated with La Niña. Extreme and anomalous hydrometeorological events, such as those following tropical storm Cristobal in 2020, revealed the fragility of Bacalar Lagoon, causing a notable transformation in lake color and transparency, shifting it from its typical oligotrophic state to eutrophic conditions that lasted longer than a year. These color changes raise questions about the factors impacting ecological health in tropical karstic regions. Additional factors affecting water quality in the BL in 2020, such as deforestation, coastline changes, and urban growth, warrant further investigation. Our study can serve as a starting landmark.

Keywords: bathymetry; seasonality; interannual; tropical storms; aquifer; ENSO; submerged dolines

1. Introduction

Approximately 13.1% of all carbonate rocks (karst) occur in tropical climates, including the Yucatan Peninsula and Florida, the world's largest coastal and lowland karst regions [1]. Due to the karstic nature of the Yucatan Peninsula, freshwater lakes are relatively rare, in contrast to water systems in sinkholes, caves, and dissolution channels [2,3].

Within the karstic terrain of the Yucatan Peninsula, the Bacalar Lagoon (hereafter referred to as BL) emerged as one of the most important tropical freshwater ecosystems within such landscapes. Tropical lakes represent approximately ten percent of the total

lakes worldwide [4]. However, the physics of tropical lakes and reservoirs is less studied than that of non-tropical lakes [5–7], particularly tropical karstic lakes.

BL is the largest freshwater lake in the Yucatán Peninsula and the second largest in Mexico. It is 50 km long and approximately 60 km from the sea coastline, framed by Chetumal Bay and the Mexican Caribbean. It is indirectly connected to Chetumal Bay, considered an estuary [8], through the Hondo River, the only surface river in the Yucatan Peninsula, as well as by a system of minor lagoons in the northeast [9]. BL presents different tonalities of blue when the insolation is high; thus, it is locally known as the “Laguna de siete colores” (lagoon of seven colors). The blue colors are associated with its oligotrophic condition, low nitrate concentrations [2], phosphorus concentrations below the detection threshold (pers. obs.), and a relatively high Secchi transparency of more than 10 m [10].

The presence of gigantic microbialites, the largest worldwide, spanning approximately 10 km in the southern part of the system, due to concentrated groundwater discharges with specific chemical conditions favoring their growth, deserves attention [11–14]. They are also among the most diverse in microbial composition [13,14]. In addition to the microbialites, this lake is a habitat of unique biodiversity, including phytoplankton [12]; mussel-like bivalves [15]; distinctive species of zooplankton, including acari [16,17]; lake flies [18]; birds [19]; and 57 fish species [20]. Some of these life forms are considered endemic to this region. Therefore, it is considered the most important epicontinental aquatic system in the Yucatán Peninsula. Moreover, this ecosystem is not connected directly to the sea, but is considered an “extreme” freshwater environment due to the high concentrations of HCO_3 (2.70 meq) and SO_4 (22.21 meq) [2].

Despite the remarkable geological, ecological, and environmental relevance of BL, as demonstrated by the publications referenced here, there remains a gap in understanding its basic limnology and the utilization of in situ measurements. Mainly, bathymetric information remains unknown and the role of the hydrometeorological regime on its dynamics is also unexplored. The analysis of the morphology and hydrometeorological conditions represents a first and crucial step in understanding basic lake hydrodynamics, the effects of which are distinctively related to physical, chemical, and biological processes that integrate the lake’s metabolism [21–23]. Moreover, while sinkholes (known locally as cenotes) and caves have garnered extensive attention and intensive research, lakes, on the other hand, remain comparatively understudied and comprehensive information is lacking.

From 30 May to 8 June 2020, the tropical storm Cristobal (previously named tropical storm Amanda in the Pacific Ocean) migrated from the Pacific Ocean, passing through Guatemala and Campeche, on the western side of the Yucatan Peninsula. This sui generis tropical storm significantly affected the region, including the states of Campeche, Chiapas, Quintana Roo, Tabasco, Oaxaca, Veracruz, and Yucatán [24]. After the tropical storm Cristobal stroked with unprecedented rainfall on the west coast of the Yucatán Peninsula at the beginning of June 2020 [25], approximately 66% of the lagoon changed its color from blue to brown-green, lasting up to nine months [26], an unmatched change that exposed its fragility. Furthermore, in recent years, BL has become an international tourist destination in a disordered way and without clear urban development plans [14]. Given the remarkable environmental changes in BL, a comprehensive understanding of its morphometry, bathymetry, and hydrometeorological characteristics is critical. Therefore, this research aims to address the scarcity of information regarding the morphometry and the hydrometeorological response of this epicontinental aquatic system of the Yucatán Peninsula. Additionally, this study included an analysis of the effects of the tropical storm Cristobal on the lake, encompassing changes in color and transparency, providing unprecedented insights into this ecosystem. Furthermore, an investigation into precipitation anomalies and the El Niño–Southern Oscillation (ENSO) is incorporated.

This study contributes to the broader field of tropical karstic lake knowledge and serves as a baseline for further research to understand the intricate interplay between hydrological processes and environmental factors.

2. Materials and Methods

2.1. Study Area

BL is a tropical freshwater lake located in the southeasternmost Yucatán Peninsula that extends between 18.93854° N, 88.13498° W and 18.53929° N, 88.49178° W (Figure 1). This lake was the result of a geomorphologic formation from tectonic events during the Late Cretaceous to the Pliocene [27], over an onshore horst and graben block fault system over the Hondo River Fault Zone, which runs northeast–southwest along the eastern portion of the Yucatan Peninsula [27–30].

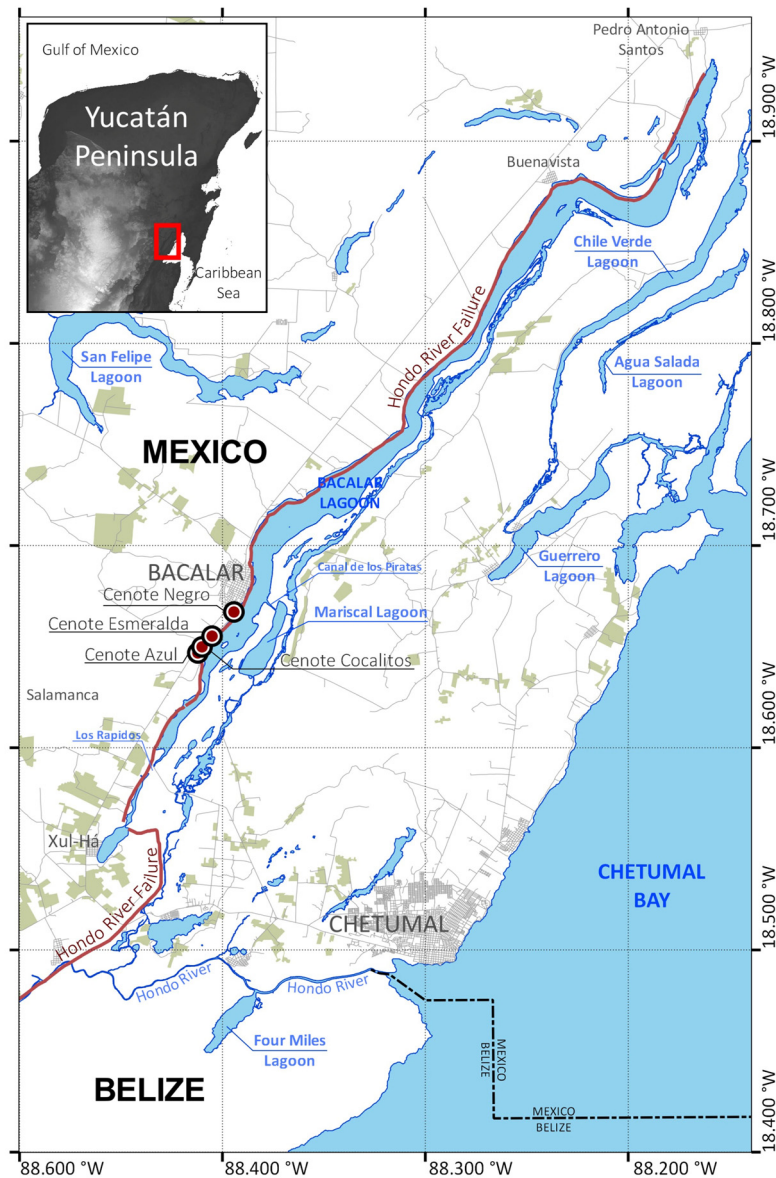


Figure 1. Study area. Locations mentioned in the text are shown. The red line corresponds to the Hondo River fault. The Yucatán Peninsula in the upper-left corner shows gray background shading, indicating relative topographic elevation, with white as the highest. The red circles show the submerged dolines, called Cenotes.

A surface current develops towards the north from Xul-Ha [2,31], flowing over intermittent flooded areas and streams that connect BL indirectly with Chetumal Bay, via the Hondo River and a system of minor lagoons in the northeast, such as Chile Verde Lagoon, Salada Lagoon, and Guerrero Lagoon (Figure 1) [9]. A direct hydrological connection with seawater is null, explained by the low chloride (Cl) content in BL, which is an extremely

hyper-carbonated environment [31–33]. The groundwater is the primary water source for BL and, accordingly, with concentrations of Ca, HCO₃, and Sr, the water originates from the western side of BL [2,31,34]. Three sub-lacustrine dolines are found within the hydrological system (from south to north: Cenote Cocalitos, Cenote Esmeralda, and Cenote Negro), with no published studies on their geomorphology. A fourth sinkhole, Cenote Azul, located 100 m from BL, is considered by some authors to be part of the BL [9,35]. However, they exhibit different water chemistry [2,36] and, consequently, a dissimilar zooplankton community [37]. Xul-Ha Lagoon is located south of BL and is directly connected to the main basin lake through a narrow channel, the southern limit of the present study area.

The system is highly oligotrophic, with low concentrations of nutrients (nitrogen and phosphate) [2]. The concentrations of phosphates are below the detection limits of 0.01 and 0.1 mg/L. However, the orthophosphate values have been reported as 0.003 mg/L ± 0.002 [38]. The pH values ranged from a minimum of 6.6 [39] to a maximum of 8.3 [40]. The northern area of BL features muddy sediments and turbid waters [41], which contrasts with the sandy bottoms of the southern area and the higher Secchi water transparency [42], with values reported at up to 10 m in depth [10].

The area is affected by the passing of tropical waves, tropical storms, and hurricanes during summer and autumn [43,44], modulating the seasonality of the precipitation in this region. A total of 151 tropical cyclones made landfall over the Yucatán Peninsula between 1851 and 2019 [45]. The rainy season in this region represents 70% of the annual total, from May to October [46], with annual mean rainfall ranging from 1107.63 to 1432.30 mm/year [47]. However, mid-summer rain decreases, causing intra-seasonal drought or heatwaves [48]. The dry season is between March and May, with the lowest precipitation and relative humidity values [8]. Climatological precipitation mean values of 25 mm have been reported for March and approximately 170 mm for September [49]. The average annual air temperature is 26.5 °C, with extreme maximum values of 39 °C [8]. However, between December and February, brief (2–5 days) cold fronts characterized by northerly winds with light rains, locally known as “nortes”, are common [50], with the lowest air temperature values being around 13 °C [8].

2.2. Bathymetry/Field Data Collection and Data Processing

Bathymetric data were collected with a LOWRANCE LCX-112c Echo Sounder (Lowrance Electronics Inc., Tulsa, OK, USA), integrated with a standard dual-frequency (50 and 200 kHz) transducer with an external Garmin Global Positioning System (GPS) antenna. The bathymetric survey was carried out from 25 to 31 August 2010, covering the entire lake at an average speed of 5 km/h, with a recording frequency of 1 Hz. The bathymetric survey was conducted along transect lines, which are perpendicular and diagonal to the shoreline. The distance between transects varied between 200 and 300 m. The total surveyed distance was 238.2 km. A total of 198,138 sounded georeferenced points were collected. No data were obtained at depths with insufficient under-keel clearance (<50 cm). The sampling site included Mariscal Lagoon in front of Bacalar town, which was connected directly to BL through a narrow channel named “Canal de los Piratas”.

Basic processing consisted of exporting the digital information recorded in the Lowrance Sonar Log Data format (.SLG) to a comma-delimited text format, using the command line executable program SLG2TXT.EXE provided by the Lowrance Customer Service department. Post-processing was applied to flag spurious points related to the loss of bottom and position. The data were then passed through an algorithm that filtered the flagged data and removed those with depths with positions repeated more than twice consecutively. After quality control, 168,454 valid georeferenced depths were spatially interpolated every 20 m, using the kriging method [51] on the Golden Software SURFER (version 9.11.947). The shoreline was digitized and georeferenced from DigitalGlobe, Cnes/Spot Image; orthophotos from the web map service from INEGI (<https://www.inegi.org.mx/temas/imagenes/ortoimagenes/#mapas>, accessed on 23 October 2023) were used. This grid was then used to build bathymetric maps using the open soft-

ware QGIS version 3.16.11., which is referenced to the UTM Zone 16Q GRS 1980 spheroid and datum ITRF 1992 (International Terrestrial Reference Frame).

2.3. Morphometric Parameters

The morphometric parameters of maximum length (m), maximum width (m), surface area (m^2), lake volume (m^3), maximum depth (m), mean depth (m), volume (m^3), shoreline length (m), and shoreline development index were obtained according to [52], by using the bathymetry data in the QGIS environment version 3.16.11. The Mariscal Lagoon was included in the morphometric description (Figure 1).

2.4. Hydrometeorological Data and ENSO

Daily rain (mm/day), relative humidity (%), and air temperature ($^{\circ}\text{C}$) data for the period of 1 January 1981–31 December 2022 (41 years) from climatological data Modern-Era Retrospective analysis for Research and Applications, Version 2 (MERRA-2) were obtained from the NASA POWER (Prediction of Worldwide Energy Resources) project (available database at <https://power.larc.nasa.gov>, accessed on 1 January 2024). The spatial resolution of the MERRA-2 data is $0.5^{\circ} \times 0.5^{\circ}$ grid cells. The selected location was latitude 18.679° N and longitude 88.39° W. Rainfall can be highly localized; thus, in situ observations from the nearby ECOSUR meteorological station, located at 18.544° N, 88.26° W, for the period of 15 February 2009–15 December 2013, were used to compare air temperature ($^{\circ}\text{C}$) and rain (mm) with the MERRA-2 data (Figure 2). The bias was calculated by subtracting the meteorological data from the MERRA-2 data for each monthly value and then taking the mean of the differences, resulting in values of -0.54°C and 20.13 mm for air temperature and rainfall, respectively. Additionally, correlation coefficient (R) values of 0.9 and 0.85 were obtained between the in situ and MERRA-2 data for air temperature and rainfall, respectively. The obtained bias and correlation coefficient (R) values demonstrate a high level of correspondence between the ECOSUR meteorological station and MERRA-2 data, providing confidence in the reliability of the dataset. It allowed us to construct the monthly climatology for air temperature ($^{\circ}\text{C}$), relative humidity (%), and rainfall (mm/month) using the 41 years of daily MERRA-2 data.

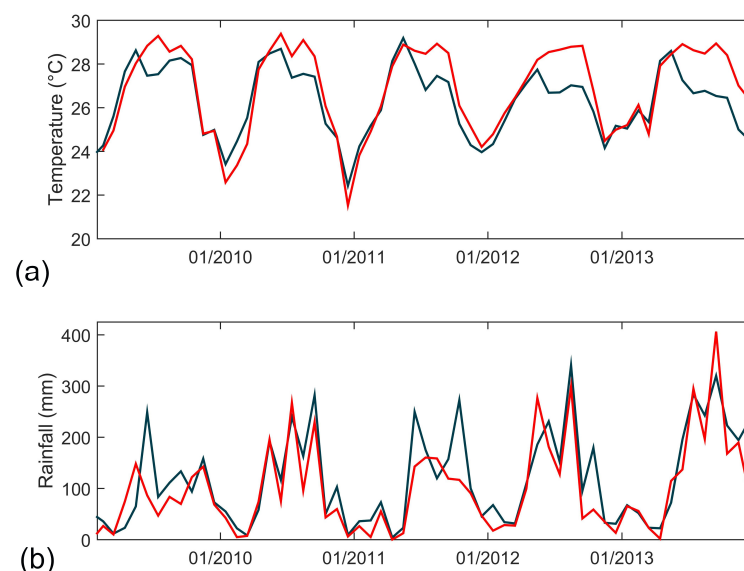


Figure 2. Time series of monthly (a) air temperature ($^{\circ}\text{C}$) and (b) rainfall (mm) from the in situ ECOSUR meteorological station (red lines) and MERRA-2 data (blue lines) for the period from 15 February 2009 to 15 December 2013.

The criteria established by the Mexican Weather Service (Servicio Meteorológico Nacional—SMN, <https://smn.conagua.gob.mx/es/>, accessed on 31 August 2021) for rain-

fall values ≥ 50 mm in 24 h were used to identify intense and heavy rain events in the local meteorological station rainfall time series from 25 May 2010 to 31 May 2012.

The monthly Rainfall Anomaly Index (RAI) was calculated, to analyze the intensity of the dry and rainy months. The RAI was established in [53], as follows:

$$\text{RAI} = 3 \left[\frac{N - \bar{N}}{\bar{M} - \bar{N}} \right] \text{ for positive anomalies} \quad (1)$$

$$\text{RAI} = 3 \left[\frac{N - \bar{N}}{\bar{X} - \bar{N}} \right] \text{ for negative anomalies} \quad (2)$$

where N is the monthly rainfall, \bar{N} is the average rainfall of the historical time series, \bar{M} is the average of the ten highest monthly rainfall values, and \bar{X} is the average of the ten lowest monthly rainfall values.

Monthly values of the Multivariate El Niño–Southern Oscillation Index version 2 (MEI) (available at <https://psl.noaa.gov/enso/mei/>, accessed on 7 March 2023) for 2000–2022 were used to identify El Niño/La Niña events and to compare them to the monthly RAI information. MEI version 2 is an updated version of the original MEI [54,55] and utilizes data from sea level pressure, sea surface temperature, surface zonal winds, surface meridional winds, and outgoing longwave radiation over the tropical Pacific basin (30° S–30° N and 100° E–70° W) to generate a time series of El Niño–Southern Oscillation (ENSO) conditions from 1979 to the present. Positive MEI values represent El Niño conditions (the warm phase of ENSO), while negative MEI values represent La Niña conditions (the cold phase of ENSO) [54,55].

2.5. In Situ Water Temperature, Water Level Records, and Derived Water Storage Anomaly

Hourly temperature and water level data were obtained from a HOBO Water Level Logger U20-001-01 installed at 18.649° N, 88.411° W from 25 May 2010 to 24 May 2012. Water temperature was measured from 25 May 2012 to 30 January 2013 using a HOBO Water Temp Pro v2 at the same site. An optimal 12-point running average low-pass filter was applied to the recorded mean daily air temperature (°C), water temperature (°C), and water level (m) data to reduce noise. The mean water level was obtained by subtracting the mean value from the water level time series.

As a first approximation to examine seasonality, Fourier curve fitting was applied to both the water temperature and water level time series [56]. This approach involved the utilization of annual and semi-annual frequencies. Fitted coefficient estimates with 95% confidence intervals and goodness-of-fit statistics such as R-squared and root mean square error (RMSE) are presented. The Pearson correlation coefficient was calculated between air and water temperature, and the significance criterion was set at $p < 0.05$.

Additionally, the Water Storage Anomaly monthly data from April 2002 to May 2023 for the Yucatán Basin, derived from satellite gravimetry within the Gravity Recovery and Climate Experiment (GRACE) missions, were considered proxies for groundwater storage. This derived product is hosted in the HydroSat dataset by the Institute of Geodesy (GIS) at the University of Stuttgart [57] and can be accessed at <http://hydrosat.gis.uni-stuttgart.de> (last accessed on 2 September 2023). HydroSat offers time series information on terrestrial water storage anomalies for major hydrological basins and at $0.5^\circ \times 0.5^\circ$ grid cells. This GIS product is based on the ITSG-Grace2018 unconstrained gravity field model that was developed by the Institute of Geodesy at Graz University of Technology [58,59]. HydroSat basin number 317 is the Yucatán Basin, which is centered at 19.63° N, 89.23° W, covering an area of 81,547.77 km². Although GRACE estimates have a bias in the estimation of the monthly amplitude [60], the monthly Water Storage Anomaly data (in meters) were compared with in situ measurements of the Bacalar water level from the HOBO Water Level Logger U20-001-01, for the analyzed periods of 25 May 2012 to 30 January 2013, as well as 26 March 2022 to 15 July 2023. The Pearson correlation coefficient was calculated between the water level time series. As a preliminary approach, an extrapolation of the

time series between in situ and satellite water levels was performed using a polynomial linear regression.

To analyze the relationship between the seasonal behavior of precipitation and the Water Storage Anomaly, the monthly precipitation time series envelope was calculated using a window size of 6 and was then correlated with the Water Storage Anomaly during the period of January 2002 to December 2020.

2.6. Transparency from Secchi, Aerial Photographs, and Sentinel-2 L1C True Color Images

To compare and analyze the evolution of transparency, particularly after tropical storm Cristobal (1–10 June 2020), historical in situ Secchi disk measurements (1997–2021) were used. Secchi depth measurements were obtained at 18.6506° N, 88.4094° W. Additionally, aerial photos taken with a Mavic 2 drone at two BL sites, one located at a northern site (18.8646° N, 88.2466° W) and the other at a southern site (18.6776° N, 88.3885° W), are presented. Northern site photos were taken on 4 March 2019, 21 July 2020, 20 October 2020, and 19 June 2021 under clear–partially cloudy sky conditions and at an altitude of approximately 60 m. Southern site photos were obtained on 4 March 2019 and 20 July 2020 under clear–partially cloudy sky conditions and at altitudes of approximately 100 and 150 m, respectively. Given the limitations of light conditions during the flight, to support visual inspection of the photos, a qualitative color comparison among the aerial photos at the northern site was performed. First, each photo was georeferenced and then a rectangle with an area of 375 m² was obtained, with a 0.05 m pixel resolution. Since each pixel in an image has 3 bytes of red, green, and blue (RGB) color information, one pixel can be represented as (0–255, 0–255, 0–255). Therefore, the histogram of the RGB channels of the photo was obtained.

Additionally, to examine changes in the area of BL both before and after the Cristobal Storm, Sentinel-2 Optimized L1C True Color images from <https://dataspace.copernicus.eu/> (last access: 24 June 2023) were used. However, cloud cover is a limitation when using optical images in tropical regions. Therefore, we selected available images within a period close to the drone flights. These images presented less than 30% cloud cover, corresponding to 14 February 2019 and 13 July 2020. The selected area covers Bacalar Lagoon and the northeastern lagoons of Chile Verde, Salada, Guerrero, and the northern area of Chetumal Bay. The northernmost and westernmost point is located at 18.9375° N and 88.5042° W, while the southernmost and easternmost point is at 18.6524° N and 88.0012° W.

3. Results

3.1. Bathymetry and Morphometric Description

The morphometric parameter values of the BL are shown in Table 1, while the bathymetric features are presented in Figures 3–6. BL is a highly elongated lake with a shoreline development index of 6.19. It extends 52.7 km from the northernmost point at Pedro Antonio Santos to the channel connecting with Xul-Ha lagoon, the southernmost limit in this study (Figure 1). The mean depth is 8.85 m and the width is variable (0.18–2.28 km), with a mean of 1.54 km. The estimated surface area is 59.1 km² and the total volume is 554.4 million cubic meters (Table 1). The hypsometric curve and the relationship between depth and percentage cumulative volume are presented in Figure 3. The surface area–depth relationship (hypsometric curve, red line) showed a basin shape with a gentle slope (6.67%) for the first 2.0 m depth. Afterward, BL showed a steeper slope of 30%, between 3 and 23 m depth. Approximately 50% of the volume is found at 6.4 m depth, and nearly 90% is contained between 0 and 15.5 m. Even when the main BL basin can be considered as a relatively deep water body, one-third of the lake surface area (according to the hypsographic curve) has water depths < 3 m.

Table 1. Morphometric parameters of the main body of Bacalar Lagoon and of Mariscal Lagoon.

	Main Body	Mariscal Lagoon
Maximum length (m)	52,667	4464
Surface Area (Ao) (m ²)	59,127,235	3,352,366
Shoreline length L (m)	168,861	10,870
Shoreline development index (DL)	6.19	1.67
Mean depth (m)	8.85	5
Maximum depth (m) *	26	17.7
Lake volume (m ³)	554,398,900	16,655,607

* Cenotes are not included.

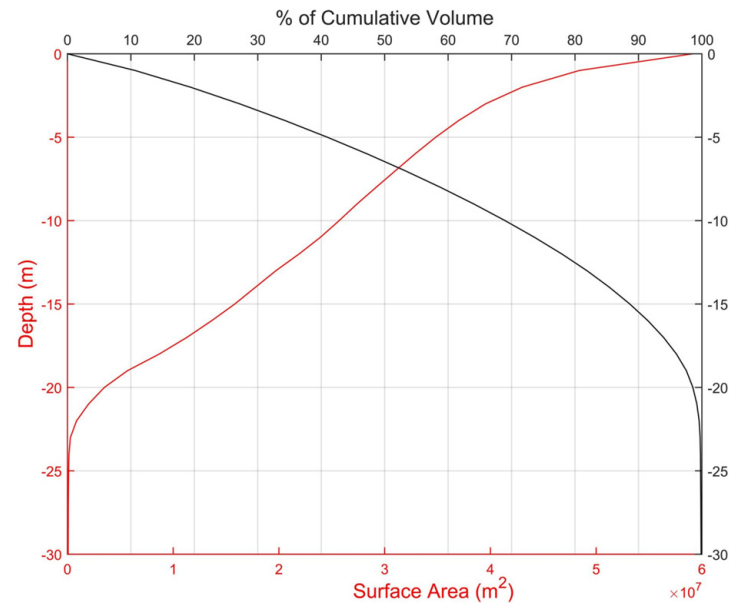


Figure 3. Hypsographic curve (red line) and percentage of cumulative volume (black line) of Bacalar Lagoon.

The bathymetric map was divided to support a more detailed visualization of the depth contours into the northern part, here referred to as Buenavista (Figure 4a), and the southern portion, here referred to as Bacalar Town (Figure 4b). Its major axis lake is oriented 35° NE. However, in the north, the BL basin configuration showed an elbow-like form around Buenavista (see Figure 1), where the lagoon is perpendicular to the central axis (Figure 4a).

The deepest bottom values are observed in the northern portion of BL, reaching 26 m (Figure 4a). In front of Bacalar Town is an eastward embayment called Mariscal Lagoon, with an area of 3.2 km² and a water depth of up to 17 m (Figure 4b). It is connected to BL by a narrow and shallow channel known as “Canal de los Piratas”, which is 780 m long, 30 m wide, and deep below 1.0 m. However, in the center, values up to 1.8 m are reached. Contour lines, nearly parallel to the shoreline, indicate that the western side has a steeper slope than the eastern side of the BL (for instance, 9% vs. 4%). The deepest part of the lake basin is not aligned at the center; instead, it is found toward the western side.

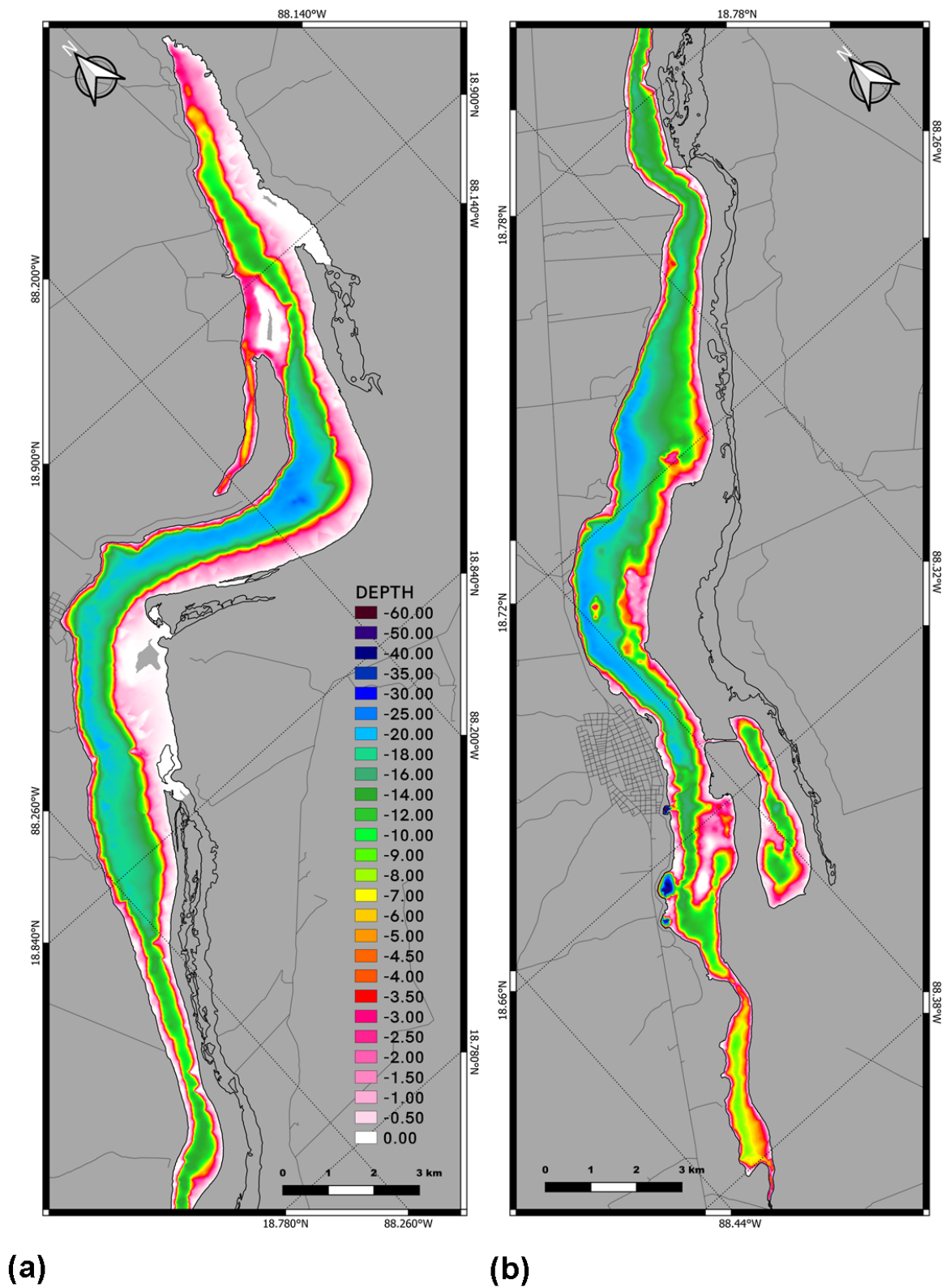


Figure 4. Bathymetric map of Bacalar Lagoon’s main basin. The values of the level curves are given by the color scale. Depth in meters. (a) Northern section of BL, (b) southern section of BL.

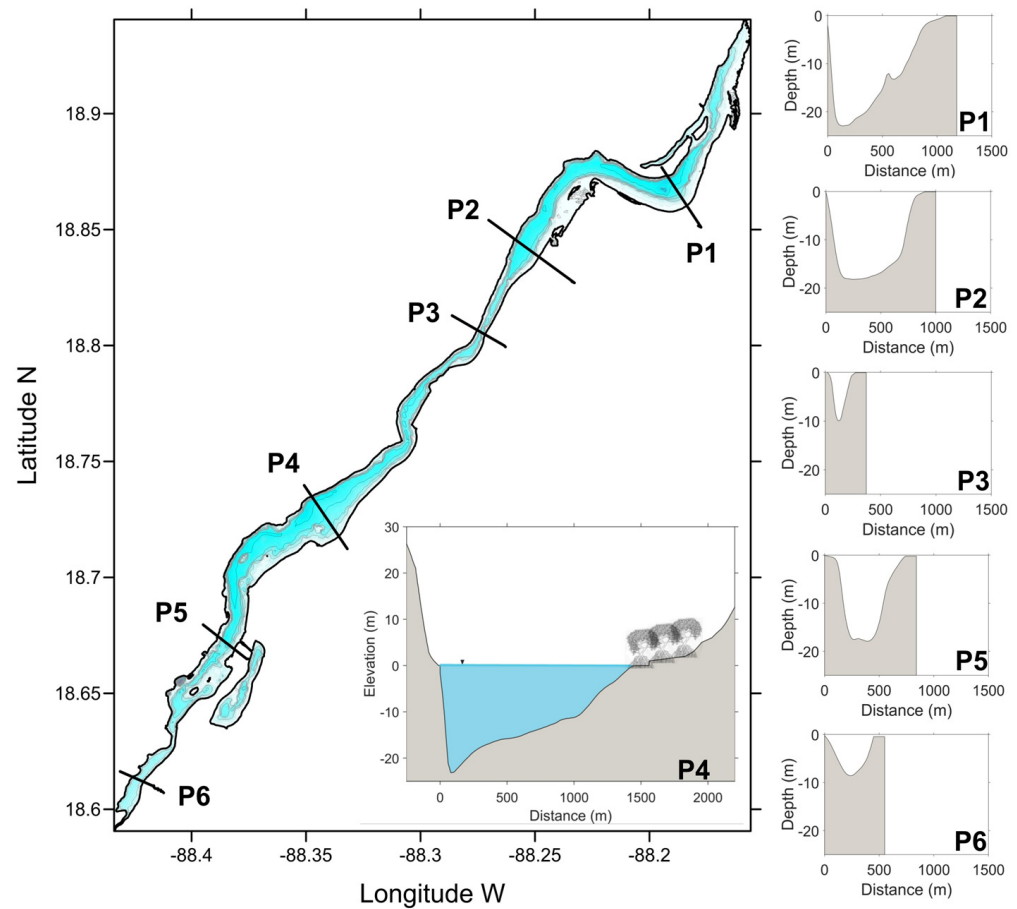


Figure 5. Transverse profiles of typical cross sections along Bacalar Lagoon's main basin. Profile P4 includes coastal elevation (m). Coordinates centered at the center of the cross section: P1, 18.86719° N, 88.18827° W; P2, 18.8422° N, 88.25366° W; P3, 18.80577° N, 88.27345° W; P4, 18.72816° N, 88.34278° W; P5, 18.67161° N, 88.38439° W; P6, 18.61289° N, 88.42318° W.

Figure 5 presents cross-sections showing distinct basin profiles along the lake. The pronounced steepness of the western side of BL is prominently visible in sections P1, P2, and P4. Lakeside elevation steepness is shown in the profile of P4, highlighting the depth variations in the bathymetry of the western coast, demonstrating the continuity of the terrain profile. The deepest values are observed inside the three aligned sub-lacustrine dolines or sinkholes on the western coast, close to Bacalar town (Figure 1).

Details of the morphology of these sub-lacustrine features are shown in Figure 6. These submerged cenotes are characterized by an almost elliptical rim and steep sidewalls beneath them, forming a nearly conical basin; their dimensions varied. Cenote Esmeralda is the largest of these submerged dolines, with a minor axis (A) of 474 m, a major axis (B) of 665 m, and a depth of 48.5 m, containing a volume of 4,290,810 cubic meters. Cenote Cocalitos presented the smallest dimensions, with a minor axis (A) of 175 m, a major axis (B) of 178 m, and a depth of 38.0 m, containing a volume of 719,206 cubic meters. Cenote Negro is the deepest, with a recorded depth of 63.6 m; however, this cenote has a less-conical-shaped basin, with a minor axis (A) of 146 m, a major axis (B) of 201 m, and its volume is 790,260 cubic meters. The eccentricity values were 0.7, 0.2, and 0.68 for Cenote Esmeralda, Cenote Cocalitos, and Cenote Negro, respectively.

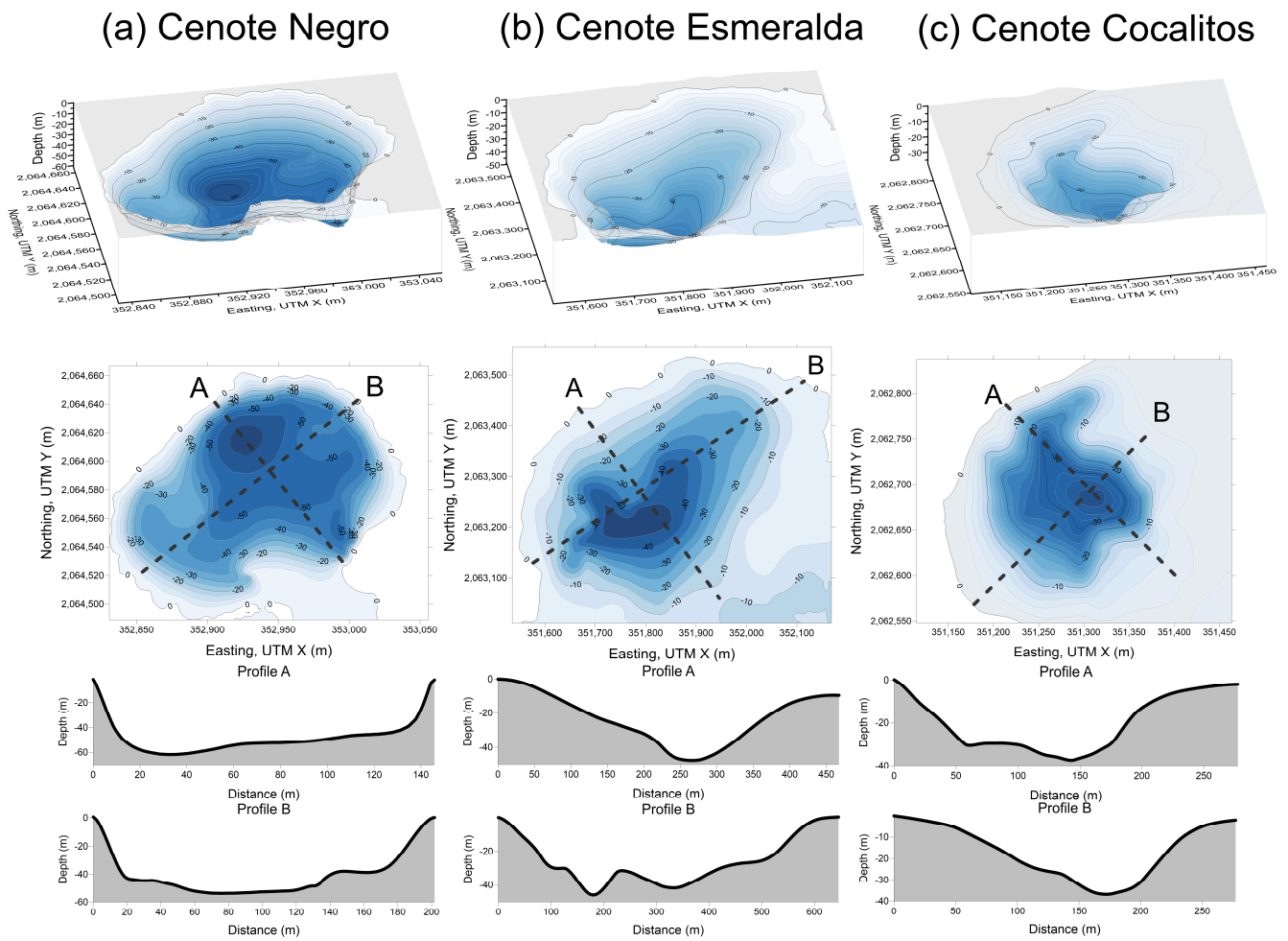


Figure 6. Bathymetric details of the three submerged dolines in Bacalar Lagoon from left to right: Cenote Negro (18.6672° N, 88.3945° W), Cenote Esmeralda (18.6549° N, 88.4050° W), and Cenote Cocalitos (18.6500° N, 88.4096° W). The top panels show the three-dimensional structure of the Cenote, the central panels show the detailed bathymetry (m) and the contours are every 5 m for Cenote Negro and Cenote Esmeralda, but every 2 m for Cenote Cocalitos. The bottom panels show the cross-sections of the minor axis (A, dashed line in the bathymetric map) and major axis (B, dashed line in the bathymetric map) for each Cenote. The depth and northing/easting coordinates (UTM16N) are given in meters.

3.2. Hydrometeorological Variability and Its Effects on Water Temperature and Water Level

The obtained annual cycle of the monthly mean values is shown in Figure 7. Their basic statistical values are shown in Table 2. The annual mean air temperature is 26.7°C , while the seasonal mean air temperature curve shows values ranging from 24.3 to 28.4°C (Figure 7a). However, higher values can be expected, with April–May being the hottest months (31°C) and the lowest air temperature occurring during December–January (16.5°C). Lower values of relative humidity (Figure 7b) are present during March, April, and May, with April having the lowest value (70%), corresponding with the dry season with low rainfall values (Figure 7c). Nonetheless, the lowest rain values were obtained during March (mean of 1 mm/day). The wet season showed two peaks, one during June (6.2 mm/day) and the second during September (6.4 mm/day).

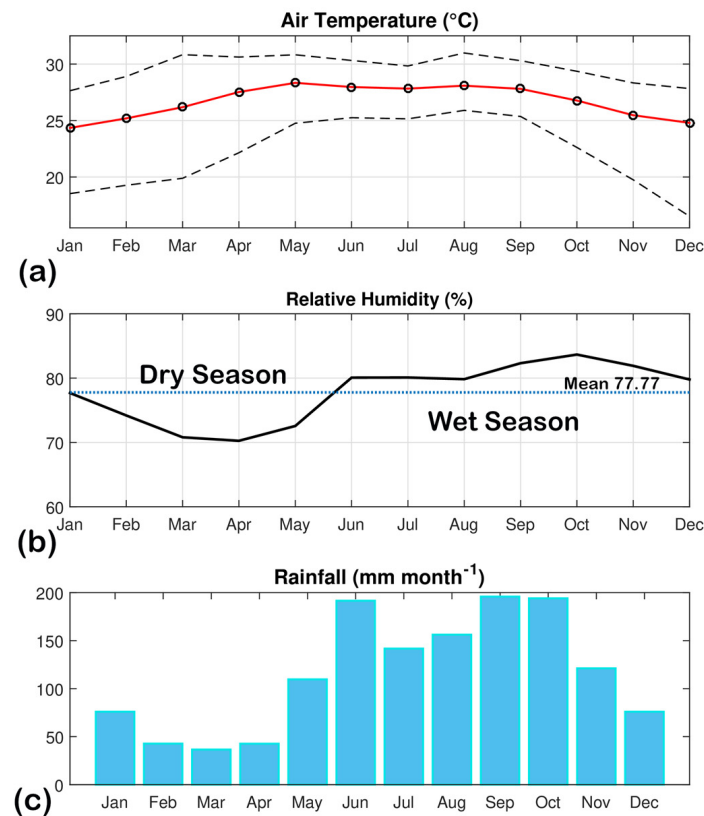


Figure 7. Climatology estimated from 41 years of MERRA2 data (January 1981–31 December 2022) of (a) air temperature (°C), monthly mean (solid red line), with minimum and maximum values (dashed lines); (b) relative humidity (%) (dotted line indicates the mean relative humidity value of 77.77); and (c) rainfall (mm/month).

Table 2. Basic statistics of air temperature (°C), relative humidity (%), daily rainfall (mm/day), and monthly rainfall from the MERRA-2 data for the period of 1 January 1981–31 December 2022.

Variable	Mean	Standard Dev.	Maximum	Minimum
Air temperature (°C)	26.7	1.8	31.0	16.5
Relative humidity (%)	77.8	7.4	95.8	42.9
Daily rainfall (mm/day)	3.7	8.3	153.7	0.0
Monthly rainfall (mm/month)	109.2	57.9	187.8	34.6

Records of daily air temperature (°C), water temperature (°C), water level (m), and cumulative daily rain (mm) are shown in Figure 8a–d. Water temperature correlates with the air temperature (Figure 8a,b), with a Pearson’s correlation coefficient of 0.89. A zero-lag correlation was obtained. The highest temperature values were recorded during the months of June–September, with values up to 30.5 °C and 30.8 °C for air and water, respectively. Minimum values were observed between November and January (the “nortes” season), when the air temperature decreased to 10 °C from that registered during the dry and rainy seasons, when minimum values of 20.5 °C and 25.2 °C for air and water, respectively, were reached. There is a clear seasonal behavior in both air temperature and water temperature. The Fourier fit curves for both the water temperature and water level series are shown in Figure 8b,c. The water temperature showed a good fit to an annual curve, with an R-square of 0.80 and an RMSE of 0.54 °C. There is higher variability in the water level data. The water level fits fairly well using the annual and semiannual signals, with an R-square of 0.62 and an RMSE of 0.036 m.

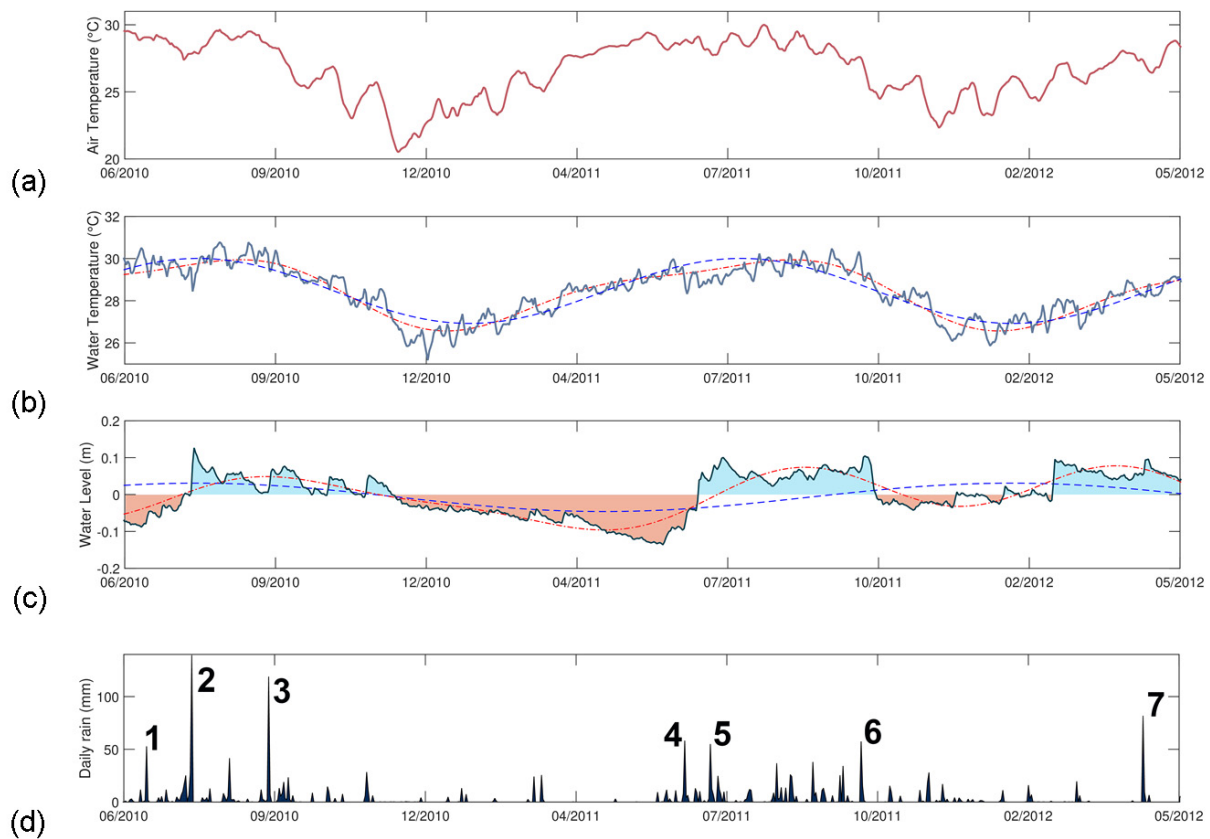


Figure 8. Time series for the period from 25 May 2010 to 31 May 2012 of (a) daily air temperature (°C) and (b) daily water temperature (°C) (gray line), fitted Fourier annual curve (blue dashed line), and fitted Fourier annual and semi-annual curve (red line). (c) Daily water level (m) (gray line), fitted Fourier annual curve (blue dashed line), and fitted Fourier annual and semi-annual curve (red line). Positive water level values are shaded in blue, while negative water level values are shaded in red. (d) Daily rainfall. Events with precipitation above 50 mm are identified and labeled: (1) Hurricane Alex (26 June 2010—51.49 mm); (2) Tropical Wave 18 (26 July 2010—138.32 mm); (3) Hurricane Karl (15 September 2010—118.80 mm); (4) Tropical Wave 3 (18 June 2011—58.22 mm); (5) Tropical wave 4 and influence of tropical storm Arlene (5 July 2011—55.53 mm); (6) Cold front 6/remains of tropical depression 12-E (13 October 2011—56.20 mm); and (7) Cold front 45 (17 April 2012—81.11 mm).

Although the relationship between water level (Figure 8c) and precipitation (Figure 8d) is not direct, some interesting patterns emerge. In BL (Figure 8c), the registered water level exhibited values above the mean during the rainy season (Figure 8d), whereas lower mean levels were observed during periods of low precipitation. BL reached its lowest level of -0.136 m on 30 May 2011, after which the water level showed a constant increase reaching 0.06 m on 30 June 2011. An increase of 0.196 m was produced in one month, defining the transition between the dry and wet seasons (Figure 8d). During the in situ water level observation period, events with precipitation greater than 50 mm/day were flagged on the daily rain plot (Figure 8d). These occurrences were identified as tropical storms, hurricanes, cold fronts, and tropical waves, through an examination of historical bulletins and weather reports provided by the Mexican Weather Service (Servicio Meteorológico Nacional—SMN, <https://smn.conagua.gob.mx/es/>). Notably, not all rainfall events led to significant increases in the water level. Nevertheless, peaks in the water level were observed for each significant weather phenomenon. For instance, on 26 July 2010, during the passage of tropical wave #18, a substantial rainfall event of 139.4 mm within a single day resulted in a water level peak, with an increase of approximately 0.13 m.

Figure 9a presents two decades (2002 to 2022) of monthly Water Storage Anomaly data for the Yucatan Basin, derived from GRACE products. In addition, it includes in

situ water levels (m) for Bacalar Lagoon. Despite some differences between the series, the monthly Water Storage Anomaly exhibited a very close resemblance to the in situ water level (Figure 9a). Although the in situ observation period is relatively short, the Pearson correlation coefficient between the in situ observations and the satellite product is 0.89. The extrapolation of the in situ water level time series, using the Water Storage Anomaly data, based on their high correlation, revealed that there was a rapid change in the water level in BL between April 2020 and July 2020.

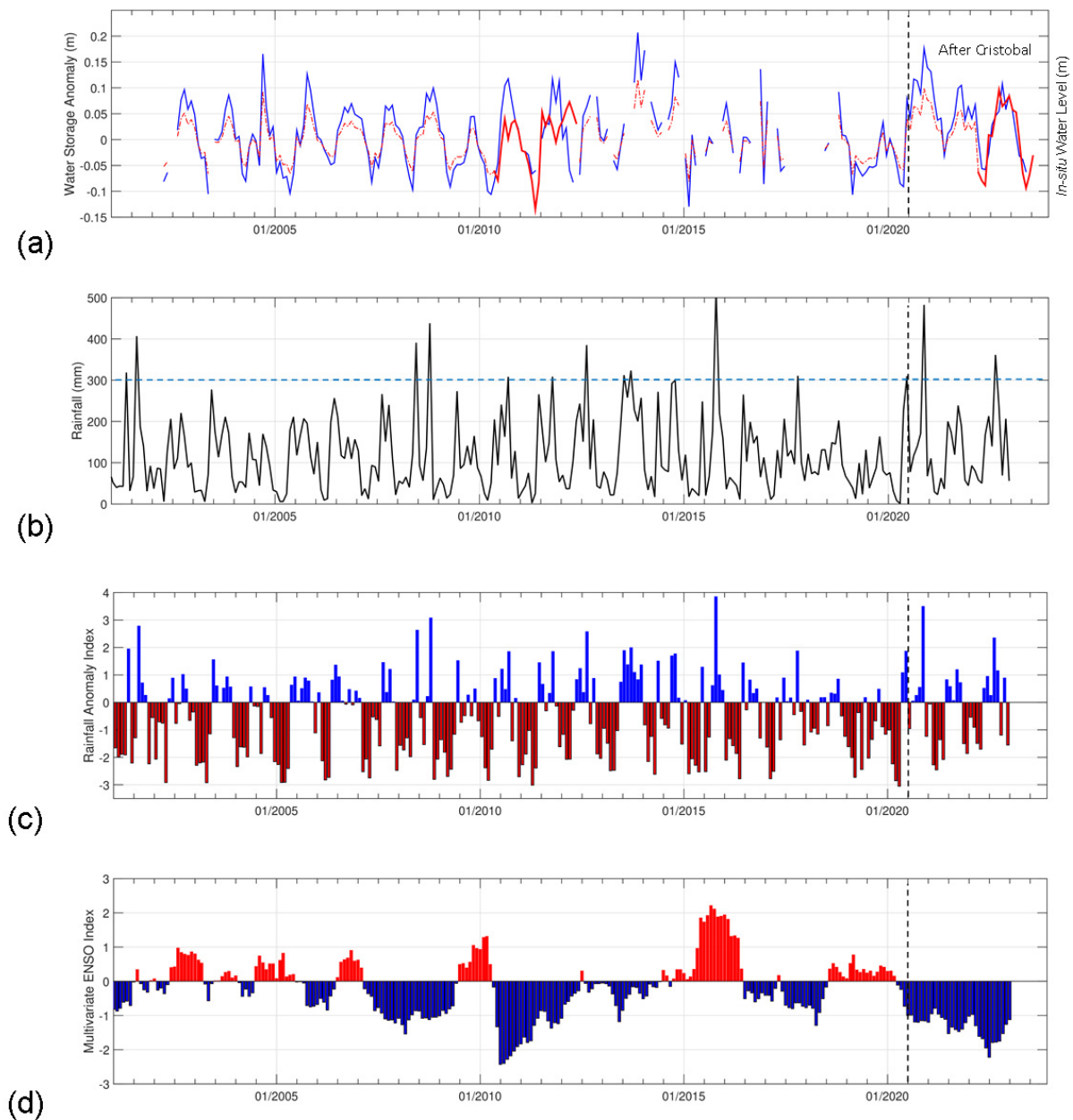


Figure 9. (a) Monthly Water Storage Anomaly (m) for the Yucatán Basin time series (blue line) and in situ water level (m) for Bacalar Lagoon (red line). The red dashed line represents the reconstructed water level (m) at Bacalar Lagoon. (b) Monthly rainfall (mm); the dashed line indicates 300 mm. (c) Monthly Rainfall Anomaly Index (RAI), blue bars represent positive anomalies, while red bars represent negative anomalies. (d) Multivariate El Niño–Southern Oscillation (ENSO) Index (MEI). Positive MEI values in red represent El Niño events. Negative MEI values in blue represent La Niña events.

Figure 9b shows the monthly rainfall time series during the same period as the Water Storage Anomaly. A significant relationship is observed between the seasonal behavior of precipitation and the Water Storage Anomaly, with a Pearson's correlation coefficient of 0.78 and a lag of two months. Figure 9b shows that there is interannual variability in rainfall. There are years with significant amounts of rain (>300 mm, which is approximately the mean value plus three times the standard deviation value), such as 2001, 2008, 2012, 2013, 2015, and 2020. Figure 9c depicts the monthly Rainfall Anomaly Index (RAI). From 2000 to 2022, RAI values above 3 (indicating extremely wet conditions) occurred during October 2008, October 2015, and November 2020. Severely dry conditions (RAI values less than -3) were observed in April 2011 and April 2020 (Figure 9c). Furthermore, it is clear that for most of the period of the in situ water level observations, which ranged between October 2010 and June 2011, as well as between November 2011 and March 2012, precipitation was consistently below its mean climatological value, with the lowest anomaly (RAI = -2.66) occurring in December 2010.

Figure 9d presents the Multivariate El Niño–Southern Oscillation Index (MEI). The identified extraordinarily wet years coincided with ENSO years. Specifically, the year 2015 was marked by El Niño conditions (the warm phase of ENSO), while the years 2001, 2008, 2012, 2013, and 2020 were characterized by La Niña conditions (the cold phase of ENSO). In particular, negative MEI values (La Niña conditions) were observed during the in situ observation period, which spanned from May 2010 to May 2012.

3.3. Effect of Tropical Storm Cristobal on Transparency and Color

The evolution of the BL water transparency and color after tropical storm Cristobal is shown in Figures 10 and 11. Previous historical Secchi depth transparency data showed a mean value of 5.6 m, with a maximum of up to 6.43 m and a minimum of 4 m (Figure 10a). After tropical storm Cristobal, Secchi's depth decreased to 1.72 m and the lake started to recover to the previous storm conditions, 12 months later.

Figures 10b and 11a–d show a sequence of aerial photos taken from southern (in front of Bacalar Town) and northern (near Buenavista) sites of BL, showing the color conditions of BL before and after the tropical storm Cristobal. Albeit with occasional cloud cover, Sentinel-2 LC1 images of true color for the northern Bacalar region are presented in Figure 10c. The area encompassed the lagoons Chile Verde, Salada, and Gerrero, as well as the northernmost tip of Chetumal Bay.

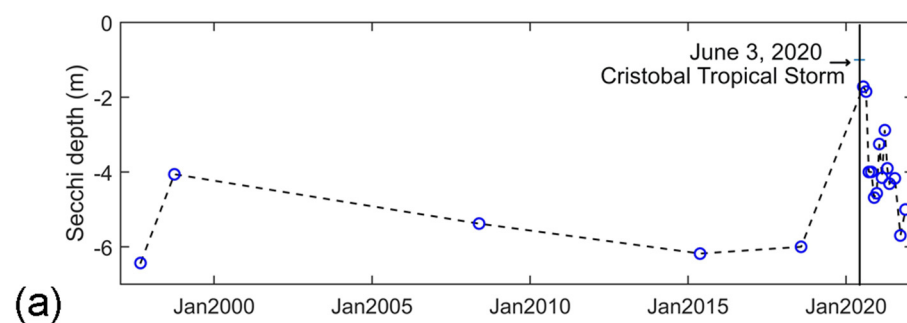


Figure 10. Cont.

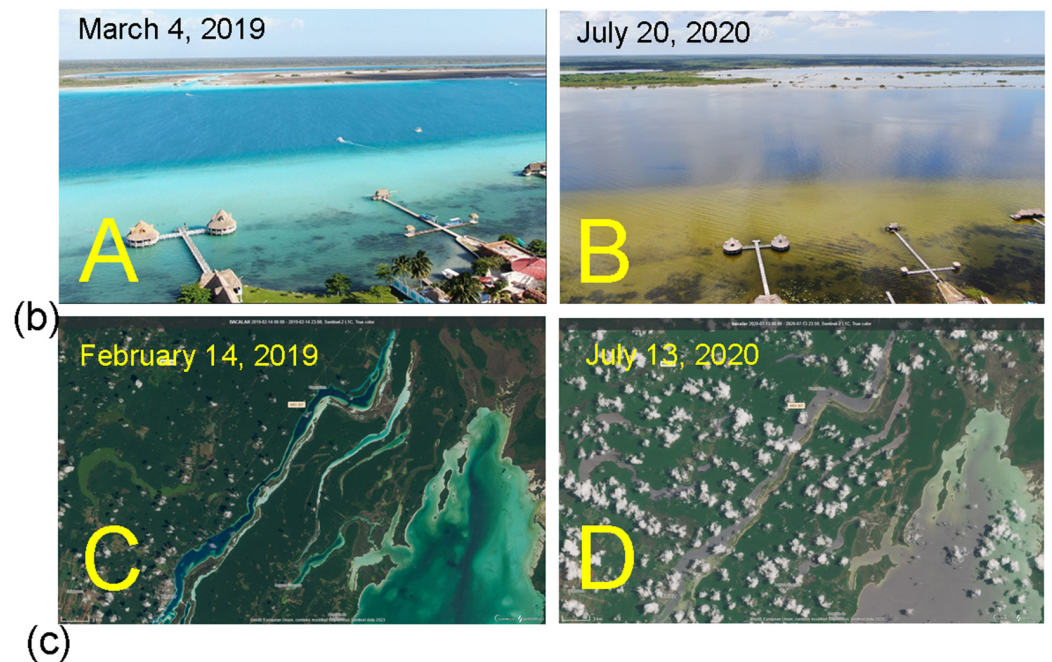


Figure 10. (a) Historical Secchi disk measurements (1997–2021), depth in meters. (b) Aerial photographs taken with a Mavic 2 drone from the southern site at 18.6776° N, 88.3885° W (Bacalar Town) on 4 March 2019 (A) and 20 July 2020 (B). Sentinel-2 Optimized L1C True Color images covering Bacalar Lagoon and the northern lagoons of Chile Verde, Salada, Guerrero, and the northern area of Chetumal Bay. The dates correspond to 14 February 2019 (C) and 13 July 2020 (D). Images with less than 30% cloud cover were included.

Before the Cristobal storm, the Bacalar basin showed a relatively consistent blue color (Figure 10b(panel A),c(panel C) and Figure 11a). However, after the Cristobal event in June 2020, significant and noticeable changes occurred in the color of the water bodies, including those of Bacalar and the western side of Chetumal Bay. They shifted from blue to a brownish hue (Figure 10b(panel B),c(panel D) and Figure 11b). The alteration in color persisted through 2020 (Figure 11b–d). Subsequently, by October 2020, a transition to a greenish color became evident, indicating potential changes in water quality and composition (Figure 11c). During 2021, the original blue color of BL had not yet completely recovered (Figure 11d), indicating that the water composition and appearance continued to be impacted. Figure 11 also shows the results of a qualitative analysis of the lagoon color conditions, based on the RGB histogram related to an area extracted from the aerial photos. One month after the passage of the tropical storm Cristobal (2–6 June 2020), the color of the water changed from blue–green to brown, due to the presence of a blue–green–red mixture (Figure 11b,f). The dominant blue–green signal observed during March 2019 (Figure 11a,e) decreased in intensity, while the red signal slightly increased after the tropical storm (Figure 11f–h). By June 2021 (Figure 11d), some transparency started to be observed; however, the original blue–green signals were not entirely recovered (Figure 11h).

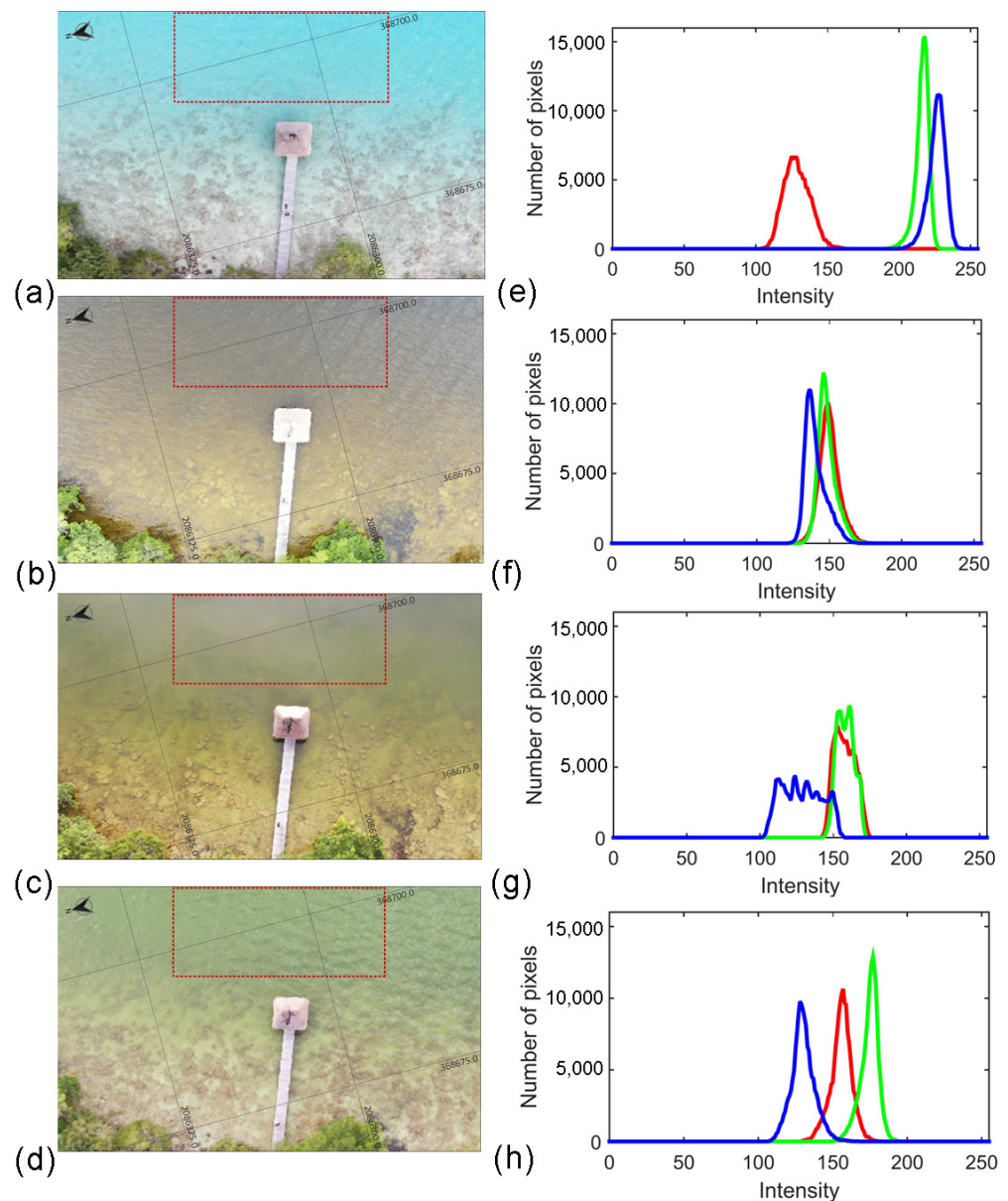


Figure 11. The left panel shows a sequence of aerial georeferenced photographs taken with a Mavic 2 drone from the northern site located at 18.8646° N, 88.2466° W (near Buenavista). (a) 4 March 2019; (b) 20 July 2020; (c) 20 October 2020; and (d) 20 June 2021. The selected area for RGB analysis is represented as a dashed red rectangle. The right panel (e–h) shows the histogram of RGB, related to the area extracted from each aerial photo. Red channel (red line), green channel (green line), and blue channel (blue line).

4. Discussion

4.1. The BL Basin as a Whole

The findings of this study provide a broader understanding of the morphometry and hydrometeorological response of Bacalar Lagoon, the largest tropical karstic lake on the Yucatán Peninsula. Examining lake morphometry is an essential component in understanding the underlying dynamics of lake hydrodynamics, a cornerstone for subsequent research in hydrology and limnology [21–23]. Basin shape often impacts overall productivity, and lake volume is vital for water-balance assessments [21,22]. Additionally, established connections exist between lake morphometry and factors such as water color, fish biomass, and phosphorus dynamics [61,62]. Before this study, the understanding of this site’s morphometry was limited and bathymetric information was absent. The existing data comprised only

basic information of surface area measurements (42.0 km²), length (40 km), and width (1 to 2 km), sourced from reports in [39,47], alongside a maximum depth of 16 m, as reported in [10]. This investigation provides comprehensive bathymetry for the entire BL, revealing significant variations in depth and extent. For example, in the northern region of BL, depths of up to 26 m have been recorded and, notably, the deepest points are within submerged sinkholes (Cenotes). The three sub-lacustrine structures, Cenote Cocalitos, Cenote Esmeralda, and Cenote Negro, are also aligned to a sinkhole, named Cenote Azul, located outside, less than 100 m from the BL [36]. The sidewalls of these features below the lake surface and the rims above it, particularly on the western side, are steep. Submerged dolines have also been observed inside Chetumal Bay, defined as blue holes, because of their marine water characteristics [63,64]. Moreover, the morphometry and bathymetry results align with well-established geological and hydrogeological information about the lake. BL's primary basin is located within a fault depression that is a recognized component of the Rio Hondo Fault zone [65,66]. This alignment is evident in its elongated shape, cross-sectional bathymetric profiles (with steeper slopes on the western side), the presence of steep escarpments along the western coast (elevating up to 20 m above sea level), and its orientation, which corresponds with the northeast-to-southwest trend of the Rio Hondo Fault Line [27,65,66].

Overall, the in situ water level of BL exhibits a strong correspondence with the monthly Water Storage Anomaly data for the Yucatan basin, derived from GRACE products. While underestimation of the monthly mean water storage variations can be expected [60], the correlation obtained allows it to serve as a proxy for the two decades of water level observations and facilitates comparison with rainfall time series. A high seasonal correlation between precipitation and Water Storage Anomaly was obtained with a two-month delay. Although there is no linear relationship between rainfall events and a direct increase in water level, a clear correlation is evident at the seasonal scale. Interannual variability in the in situ water level was observed. During most of the recorded period between 2010 and 2012, the in situ water level and rainfall were below the average (Figure 8c) and mean climatic value (RAI, Figure 9c), respectively. The scarce precipitation during the expected wet period might explain the lower water level registered in situ. Extended weather anomalies, such as exceptional drought conditions during 2010–2011, can be associated with large-scale interannual atmospheric variability. One of these is the ENSO. This phenomenon can produce strong anomalies in precipitation in this tropical area, indicating relatively wet rainy seasons [67]. However, the opposite was observed, whereby drought conditions during La Niña could affect rainfall and, thus, the water level of BL. According to the MEI values, during 2010–2012, one of the strongest and most prolonged La Niña events occurred (Figure 9d).

During 2020, according to the above historical records, 30 tropical cyclones formed in the Atlantic Ocean, 5 of which impacted the Yucatán Peninsula. These included the Cristobal and Gamma tropical storms, as well as the Hanna, Delta, and Zeta hurricanes [68]. Additionally, there were 24 cold fronts and 5 winter storms from October to December 2020. This series of storms during 2020 resulted in a significant surplus of precipitation for southeastern Mexico. That year (2020) was also a La Niña year, although it was not significantly stronger than 2010–2012. Therefore, no conclusive evidence could be drawn regarding how ENSO phenomena impact the region. For this purpose, long-term water level monitoring is needed to thoroughly investigate the effects that phenomena such as La Niña or El Niño could have on BL.

Understanding the role of hydrometeorological variability within BL is of paramount importance. Specifically, following tropical storm Cristobal in 2020, a pivotal shift occurred in the influence of extreme and anomalous hydrometeorological conditions on the health of the BL ecosystem. Nevertheless, understanding the interplay of diverse factors that impact water level and quality in BL over short periods is complex. Nonetheless, we delve into a discussion of three potential underlying drivers that could substantially contribute to the significant changes observed in BL's water color in 2020—(1) natural disturbances,

such as severe hydrometeorological events; (2) interconnectedness with the aquifer system; and (3) human-induced alterations, encompassing the deforestation of surrounding areas, coastline modifications, and urban expansion.

4.2. Natural Disturbances

The findings presented here shed light on the importance of understanding the hydrometeorological variability in BL. Weak seasonal variations in solar radiation characterize the tropics [4]. Here, it is found that there is a clear seasonal behavior in the water temperature that correlates with the air temperature, meaning that air temperature may play an important role in surface heat fluxes and the lake's thermal structure [5]. However, precipitation plays a significant role in the variability of tropical lakes [69]. Water level fluctuations in BL can be linked to weather variability. Sudden water level rise events in BL can be associated with extreme events such as tropical storms or cold fronts with rains (see Figure 8c,d). Therefore, it is expected that natural disturbances caused by major hurricanes and storms might produce important changes in the water quality of BL, as already reported for other lakes [70].

The tropical storm Cristobal, which primarily impacted Campeche state, remained stationary for three days in the southern Gulf of Mexico [24,71]. The daily rainfall in Campeche exceeded 240% of the monthly mean [71], with a maximum value of 528 mm in 24 h, reported by CONAGUA in El Carmen, Campeche [25]. In the area of Bacalar, rainfall reached only 131.5 mm [25], but after the impact of Cristobal, BL changed its color from blue-green to brown and lost its transparency, lasting up to 12 months. Moreover, the abundance of zooplankton was drastically decreased in July 2020 (M. Elías-Gutiérrez pers. obs.) and the mortality of 94,339 specimens of the native freshwater snail *Pomacea flagellate* in August 2020 was reported and attributed to the prevailing poor water quality conditions [72]. Significant alterations in the physicochemical parameters of water quality have been reported at various sites around BL following the passage of Tropical Storm Cristobal, from oligotrophic [38,73,74] to eutrophic conditions [74]. Other intense hydrometeorological events impacted the surrounding lands of BL, such as hurricane Dean (category 5) on 21 August 2007, which produced very intense winds up to 278 km/h and accumulated precipitation of 81 mm [45,75]. Dean was the most powerful storm crossing the peninsula since 1988, with a trajectory over BL [45]. Despite this extreme event having devastated large vegetation areas [76,77], no changes in water transparency or color of BL were reported, probably due to the reduced rainfall compared to other hydrometeorological events. By comparing the amount of local precipitation of tropical storm Cristobal (2020—131.5 mm) with that of hurricane Karl (2010—167 mm) [78], it could be inferred that there must be other factors in addition to local precipitation that contributed to the drastic change in the water quality of BL.

4.3. Interconnectedness with the Yucatan Aquifer System

While the complete understanding of the degree of these interconnections remains elusive, there are certain aspects that could be explored to shed light on answering the following fundamental question: Is there the possibility that changes in water level and water quality might be affected by local and remote hydrometeorological phenomena, as might be the case for the Cristobal storm, which dropped an extraordinary amount of water in Campeche [71]?

There was clear agreement between the Water Storage Anomaly monthly (GRACE product) and the in situ measured water level at Bacalar (Figure 9a). This result implies that, at least on a seasonal scale, the water level in BL responds similarly to the water storage in the Yucatan main basin aquifer (regionally). This is expected since the primary water source for BL is underground water, which gives its oligotrophic characteristics [2,31,34]. However, there are some differences, possibly because the Yucatán aquifer cannot be generalized as a single aquifer system, and the response to a hydrometeorological event may vary among the aquifer regions. The Yucatán Peninsula is situated in a region with

relatively high rainfall [45,46]; however, its landscape is described as a karst topography, devoid of surface streams or rivers [27]. The high solubility of limestone led to significant erosion before and after the Peninsula became submerged by the Caribbean Sea, generating extensive complex networks of submerged cave systems, through which groundwater flows [27,29]. An aquifer sub-system within the Yucatán Peninsula encompasses the area from the east and south of Lake Chichancanab ($19^{\circ}54'0''$ N, $88^{\circ}46'0''$ W) toward the eastern Campeche–Southeast Quintana Roo–Southernmost Yucatan [2,79], where Bacalar is located. This sub-system is characterized by slow-moving groundwater, a high sulfate content, and distinctive topography, and is referred to as the Icaiché Formation, which is also referred to as the Evaporite Region [80]. This internal interconnection between BL and Campeche is supported by a characteristic chemistry of groundwater between the southeastern and southwestern Yucatán Peninsula, which is essentially the same [79]. Furthermore, in this Evaporite Region, there are plentiful poljes, mainly attributed to the presence of a near-surface aquitard that formerly supported a perched water table that has been partially breached, resulting in a pattern of long sinuous lakes and discontinuous perennial streams [79]. Their drainage primarily occurs internally, although it may be augmented by seasonal perched surface streams that flow over dense clay layers and interconnect neighboring basins. The severity of the local precipitation over the BL area was observed from the Sentinel-2 True Color images, after the Cristobal storm (Figure 10c(panel D)) and there was a perennial interconnection between BL and the different lagoons and lakes surrounding BL. Moreover, flushing sediments from the northern lagoons (Chile Verde, Salada, and Guerrero) over northern Chetumal Bay were evident, although the main drainage to Chetumal Bay occurs through the Hondo River via the Estero de Chac narrow channels [9].

It is essential to note that during 2021 (Figure 11d), the original blue-green color signal of BL did not fully recover, implying a lasting impact on water quality. By considering the geology of the regional aquifer sub-system (the presence of a near-surface aquitard) and the fact that its groundwater flow is slow [2,79], the observed changes in the color of BL might be the result of continuous precipitation over an already saturated aquifer with slow groundwater movement. Although no water level data are available from other lakes in the Evaporite Region (e.g., Chichancanab Lake), local news and reports have shown that persistent rain has resulted in the submersion of roads and fields, particularly flood areas around Chichancanaab Lake, for several months. On 12 June 2020, after tropical storm Cristobal, the Champotón River at Campeche reported a rise level of 1.96 m above its overflow level [81].

Furthermore, local hydrological reports from Merida-Yucatan mentioned that phreatic water levels rose to 5.2 m above mean sea level after the passage of the tropical storm Cristobal, the tropical depression Gamma, and the hurricane Delta (Miguel I. Villasuso, @SUSOMID [Tweet] (8 October 2020), <https://twitter.com/SUSOMID/status/1314378212898725888>). These findings support the idea of over-precipitation (anomaly) in the region, both locally and remotely. It is likely that a combination of a slow-moving groundwater and a saturated aquifer contributed to the lasting changes in the color of BL. A study of the isotopic composition of groundwater strontium following Hurricane Isadore (in September 2002) in the northern Yucatán Peninsula aquifer sub-system indicated that several years to decades are required for groundwater to equilibrate chemically [79]. This could apply to BL; however, further investigation is warranted.

4.4. Human-Driven Alterations

The historic small town of San Felipe de Bacalar experienced an exponential growth from 24,094 to 196,766 visitors between 2008 and 2019 [82]. The rapid growth and influx of tourists in the Bacalar Lake and its surroundings drive a constantly growing urban area [83]. Services represent 31% of the economic income and 46% is due to primary activities [84,85]. The latter has produced a major change in land use [84], resulting in deforestation and greater water demand. In the last two decades, changes in land use

and land cover around BL have intensified [86]. The most affected vegetal community was the evergreen tropical forest. An estimated 36,261 ha were degraded to secondary vegetation and agricultural lands between 1997 and 2016. According to Gomez-García [84], the total coverage decreased from 17% in 1997 to only 1% in 2001. Other studies reported that up to 75,263 ha of evergreen tropical forest were lost between 1993 and 2017 [86]. In addition, a study of forest cover dynamics revealed greater degradation (12,915 ha y⁻¹) than deforestation (5882 ha y⁻¹) in the Selva Maya of Central and Southern Quintana Roo, between 1993 and 2018, where the BL region experienced the greatest net forest loss (−1.6% y⁻¹) [87].

A significant extension of wetlands surrounds the main BL water basin. All these shallow areas are subjected to desiccation during dry weather conditions. Studies reported higher electrical conductivity values in the eastern and northern parts of BL, close to shallower areas [41]. This makes BL very susceptible to climatic and anthropogenic threats. Furthermore, the shoreline development index shown in the results indicates its potential to serve as a suitable habitat for diverse wildlife and the possibility of extensive littoral human communities and activities, including tourism infrastructure (permanent or temporal) along the shores [88]. Additionally, the modification of the shoreline through the extraction of native mangrove (*Conocarpus erectus*) and the implementation of shoreline nourishment with stone materials (e.g., rip-rap embankments), to prevent erosion, further add to the environmental concerns arising from tourism development.

Furthermore, strong evidence suggests that land use has significantly impacted groundwater quality in the northern part of the Yucatán Peninsula [89], particularly in agricultural areas during the wet season. Therefore, the combination of land changes, loss of mangrove areas, urbanization, industrial tourism activities, and recreational use of the lake, along with extreme hydrometeorological events such as those observed in 2020 (including Cristobal), is likely driving the observed shift from oligotrophic to eutrophic conditions in BL.

5. Conclusions

The bathymetric data of the BL revealed it to be heterogeneous, elucidating variations in depth and extent, with a distinctive morphology that suggests its association with a geological fault, featuring submerged dolines. While the water level exhibits immediate responses to hydrometeorological events (i.e., tropical storms, hurricanes, cold fronts, and tropical waves), its responses are also influenced by seasonal dynamics that correlate with those of the regional aquifer, with a lag of 2 months after the seasonal rainfall signal. Although rainfall in this region is expected to occur during the summer, interannual rainfall variability has been present. This was associated with the ENSO, particularly La Niña events.

Incorporating the hydrometeorological behavior of these results not only advances the understanding of this unique aquatic ecosystem, but also underscores the fragility of BL to extreme and anomalous hydrometeorological events such as those that occurred after the tropical storm Cristobal in 2020. This event triggered a noticeable transformation in the lagoon's color and transparency characteristics, resulting in a departure from its usual oligotrophic state to eutrophic conditions. This change, brought about by the unusual wet conditions of that year, persisted for an extended period, stretching beyond a year. The observed changes in color raise important questions about the drivers affecting the ecological health of water bodies in tropical karstic regions. Other factors that contributed to the alteration in the water quality of BL in 2020, such as the deforestation of surrounding lake areas and changes in the coastline and urban growth, deserve further investigation, but our study can serve as a starting point.

Considering that climate change is already affecting the water cycle and increasing water-related extreme events [90], attention to our freshwater resources is critical. The intensification of storms and drought events due to climate change [90] and a lack of management plans for urban and land use changes could exacerbate the problems already

observed during 2020 in the BL. Moreover, the construction of significant infrastructure such as the “Mayan Train” will lead to the modification of the main connection channels that could severely impact water flows. This human-driven modification in the BL will aggravate water quality problems after severe weather events such as Cristobal.

As the lake’s popularity rises, thoughtful and sustainable management practices become crucial for preserving its unique ecological and cultural heritage. Decisions made by governmental development programs concerning sustainable development must consider the leading environmental aspects of the BL territory. Therefore, based on the results of this study, it is not only encouraged, but also essential to establish better strategies for maintaining the eco-hydrological balance of BL. This balance is crucial for sustaining our water resources, supporting its biodiversity and ecosystem services, and helping to mitigate the impacts of disturbances such as droughts, tropical storms, and human activities. Further research integrating the essential physical characteristics of BL with biological, chemical, and geological aspects and understanding the complex groundwater flow systems and surface hydro-connectivity in BL is urgently needed. This knowledge will be decisive in order to improve the resilience of this oligotrophic lake under the many stressful conditions it is currently facing.

Author Contributions: Conceptualization, L.C. and M.E.-G.; methodology, L.C., M.E.-G., M.Y. and M.O.N.-O.; software, data curation and visualization, L.C., M.Y. and M.O.N.-O.; formal analysis, L.C.; investigation, L.C. and M.E.-G.; writing—original draft preparation, L.C.; writing—review and editing, L.C., J.C.A.-H., O.F.R.-M., M.E.-G. and E.P.-H.; funding acquisition, L.C. All authors have read and agreed to the published version of the manuscript.

Funding: Fieldwork expenses of this research were partly funded by the Consejo Nacional de Humanidades, Ciencias y Tecnologías (CONAHCYT), and Consejo Quintanarroense de Ciencia y Tecnología grant number FOMIXQROO-2009-C01-123254, project “Monitoring of water quality from Lakes of Quintana Roo”, under Fondos Mixtos program. M.E.G. personally funded his fieldwork expenses for collecting transparency data and drone flights. The APC fees funded by El Colegio de la Frontera Sur. M.E.G. funded the acquisition of the Mavic 2 drone.

Data Availability Statement: The datasets presented in this article are not readily available, because the data belong to a project funded by the authors. Once published, data will eventually be shared on the institutional data reservoir. Requests to access the datasets should be directed to Dr. L.C., lcarrillo@ecosur.mx.

Acknowledgments: Fieldwork expenses of this research were partly funded by the Consejo Nacional de Humanidades, Ciencias y Tecnologías (CONAHCYT), and Consejo Quintanarroense de Ciencia y Tecnología grant number FOMIXQROO-2009-C01-123254, project “Monitoring of water quality from Lakes of Quintana Roo”, under Fondos Mixtos program. M.E.G. personally funded his fieldwork expenses for collecting transparency data and drone flights. Recognition is given to the CONAHCYT (National Council for Humanities, Sciences and Technologies of Mexico) program ‘Investigadoras e Investigadores por México’ (Project 761). A sincere thank you also goes out to Adrian A. Vásquez de la Mercer for his diligent proofreading of the English language of this manuscript.

Conflicts of Interest: The authors declare no conflicts of interest.

References

1. Goldscheider, N.; Chen, Z.; Auler, A.S.; Bakalowicz, M.; Broda, S.; Drew, D.; Hartmann, J.; Jiang, G.; Moosdorf, N.; Stevanovic, Z.; et al. Global Distribution of Carbonate Rocks and Karst Water Resources. *Hydrogeol. J.* **2020**, *28*, 1661–1677. [[CrossRef](#)]
2. Perry, E.; Velazquez-Oliman, G.; Marin, L. The Hydrogeochemistry of the Karst Aquifer System of the Northern Yucatan Peninsula, Mexico. *Int. Geol. Rev.* **2002**, *44*, 191–221. [[CrossRef](#)]
3. Alcocer, J.; Bernal-Brooks, F.W. Limnology in Mexico. *Hydrobiologia* **2010**, *644*, 1–54. [[CrossRef](#)]
4. Lewis, W.M. Tropical Lakes: How Latitude Makes a Difference. In *Perspectives in Tropical Limnology*; Schiemer, F., Boland, K.T., Eds.; SPB Academic Publishing: Amsterdam, the Netherlands, 1996; pp. 43–64.
5. Xing, Z.; Fong, D.A.; Yat-Man Lo, E.; Monismith, S.G. Thermal Structure and Variability of a Shallow Tropical Reservoir. *Limnol. Oceanogr.* **2014**, *59*, 115–128. [[CrossRef](#)]
6. Boon, P. The Conservation of Fresh Waters: Temperate Experience in a Tropical Context. *Trop. Limnol.* **1995**, *1*, 149–159.
7. Lewis Jr, W.M. Basis for the Protection and Management of Tropical Lakes. *Lakes Reserv. Res. Manag.* **2000**, *5*, 35–48. [[CrossRef](#)]

8. Carrillo, L.; Palacios-Hernández, E.; Ramírez, A.M.; Morales-Vela, B. Características Hidrometeorológicas y Batimétricas. In *El Sistema Ecológico de la Bahía de Chetumal/Corozal: Costa Occidental del Mar Caribe*; El Colegio de la Frontera Sur: Chetumal, Quintana Roo, Mexico, 2009; pp. 12–20, ISBN 978-607-7637-13-4.
9. Gischler, E.; Gibson, M.A.; Oschmann, W.; Hudson, J.H. Giant Holocene Freshwater Microbialites, Laguna Bacalar, Quintana Roo, Mexico. *Sedimentology* **2008**, *55*, 1293–1309. [[CrossRef](#)]
10. Pérez, L.; Bugja, R.; Lorenschat, J.; Brenner, M.; Curtis, J.; Hoelzmann, P.; Islebe, G.; Scharf, B.; Schwalb, A. Aquatic Ecosystems of the Yucatán Peninsula (Mexico), Belize, and Guatemala. *Hydrobiologia* **2011**, *661*, 407–433. [[CrossRef](#)]
11. Gischler, E.; Golubic, S.; Gibson, M.A.; Oschmann, W.; Hudson, J.H. Microbial Mats and Microbialites in the Freshwater Laguna Bacalar, Yucatan Peninsula, Mexico. In *Advances in Stromatolite Geobiology; Lecture Notes in Earth Sciences*; Springer-Verlag: Berlin/Heidelberg, Germany, 2011; pp. 187–205.
12. Siqueiros-Beltrones, D.A.; Argumedo-Hernández, U.; Hernández-Almeida, O.U. Diagnosis Prospectiva Sobre La Diversidad de Diatomeas Epilíticas En La Laguna Bacalar, Quintana Roo, México. *Rev. Mex. Biodivers.* **2013**, *84*, 865–875. [[CrossRef](#)]
13. Johnson, D.; Beddows, P.; Flynn, T.; Osburn, M. Microbial Diversity and Biomarker Analysis of Modern Freshwater Microbialites from Laguna Bacalar, Mexico. *Geobiology* **2018**, *16*, 319–337. [[CrossRef](#)]
14. Yanez-Montalvo, A.; Gómez-Acata, S.; Águila, B.; Hernández-Arana, H.; Falcón, L.I. The Microbiome of Modern Microbialites in Bacalar Lagoon, Mexico. *PLoS ONE* **2020**, *15*, e0230071. [[CrossRef](#)] [[PubMed](#)]
15. Marelli, D.C.; Berrend, R.E. New Species Record for *Mytilopsis-Sallei* (Recluz) in Central-America (Mollusca Pelecypoda). *Veliger* **1978**, *21*, 144.
16. Elías-Gutiérrez, M.; Valdez-Moreno, M.; Topan, J.; Young, M.R.; Cohuo-Colli, J.A. Improved Protocols to Accelerate the Assembly of DNA Barcode Reference Libraries for Freshwater Zooplankton. *Ecol. Evol.* **2018**, *8*, 3002–3018. [[CrossRef](#)] [[PubMed](#)]
17. Montes-Ortiz, L.; Elías-Gutiérrez, M. Water Mite Diversity (Acariformes: Prostigmata: Parasitengonina: Hydrachnidiae) from Karst Ecosystems in Southern of Mexico: A Barcoding Approach. *Diversity* **2020**, *12*, 329. [[CrossRef](#)]
18. Vinogradova, E.M. Six New Species of *Polypedilum* Kieffer, 1912, from the Yucatán Peninsula (Insecta, Diptera, Chironomidae). *Spixiana* **2008**, *31*, 277–288.
19. López-Castilla, H.; Cetzal-Ix, W.; Casanova-Lugo, F.; Ramírez-Barajas, P.; Lara-Pérez, L.; Basu, S.; Enríquez-Nolasco, J. Birdlife, a Tourist Attraction for the Southern Portion of Bacalar Lagoon, Quintana Roo, Mexico. *Braz. J. Biol.* **2023**, *83*, e275598. [[CrossRef](#)] [[PubMed](#)]
20. Valdez-Moreno, M.; Ivanova, N.V.; Elías-Gutiérrez, M.; Pedersen, S.L.; Bessonov, K.; Hebert, P.D.N. Using eDNA to Biomonitor the Fish Community in a Tropical Oligotrophic Lake. *PLoS ONE* **2019**, *14*, e0215505. [[CrossRef](#)] [[PubMed](#)]
21. Lerman, A.; Imboden, D.M.; Gat, J.R. *Physics and Chemistry of Lakes*; Springer: Berlin/Heidelberg, Germany, 1995; ISBN 978-3-642-85134-6.
22. Wetzel, R.G. *Limnology: Lake and River Ecosystems*; Gulf Professional Publishing: Houston, TX, USA, 2001.
23. Håkanson, L. The Importance of Lake Morphometry for the Structure and Function of Lakes. *Int. Rev. Hydrobiol. J. Cover. Asp. Limnol. Mar. Biol.* **2005**, *90*, 433–461. [[CrossRef](#)]
24. CONAGUA. *Presenta El Servicio Meteorológico Nacional Balance de Las Tormentas Tropicales Amanda y Cristobal*; Comunicado de Prensa No. 444-20; CONAGUA: Ciudad de Mexico, Mexico, 2020.
25. CONAGUA. *Reseña de La Tormenta Tropical Cristóbal Del Océano Atlántico*; CONAGUA: Ciudad de Mexico, Mexico, 2020.
26. Keeley, A. How a Mexican Lagoon Lost Its Colors. *New Yorker*, 12 July 2021.
27. Bauer-Gottwein, P.; Gondwe, B.R.N.; Charvet, G.; Marín, L.E.; Rebolledo-Vieyra, M.; Merediz-Alonso, G. Review: The Yucatán Peninsula Karst Aquifer, Mexico. *Hydrogeol. J.* **2011**, *19*, 507–524. [[CrossRef](#)]
28. Burkart, B. Northern Central America. In *Caribbean Geology: Introduction*; Donovan, S.K., Jackson, T.A., Eds.; The University of the West Indies Publisher's Association (UWIPA): Kingston, Jamaica, 1994; pp. 265–284.
29. Isphording, W.C. The Physical Geology of Yucatan. *Gulf Coast Assoc. Geol. Soc.* **1975**, *25*, 231–262.
30. Miller, T.E. Geologic and Hydrologic Controls on Karst and Cave Development in Belize. *J. Cave Karst Stud.* **1996**, *58*, 100–120.
31. Matzuk, R.M. Water Chemistry and Lake Dynamics of Laguna Bacalar, Quintana Roo, Mexico. Ph.D. Thesis, The University of Wisconsin-Milwaukee, Milwaukee, WI, USA, 2020.
32. Perry, E.; Velazquez-Oliman, G.; Socki, R.A. Hydrogeology of the Yucatán Peninsula. In *The Lowland Maya Area: Three Millennia at the Human-Wildland Interface*; Gómez-Pompa, A., Allen, M., Fedick, S.L., Jiménez-Osorio, J.J., Eds.; Food Products Press: New York, NY, USA, 2003; pp. 115–138.
33. Sánchez-Sánchez, J.A.; Álvarez-Legorreta, T.; Pacheco-Ávila, J.G.; González-Herrera, R.A.; Carrillo-Briebezca, L. Caracterización Hidrogeoquímica de Las Aguas Subterráneas Del Sur Del Estado de Quintana Roo, México. *Rev. Mex. Cienc. Geológicas* **2015**, *32*, 62–76.
34. Tobón Velázquez, N.; Rebolledo Vieyra, M.; Paytan, A.; Broach, K.H.; Hernández Terrones, L.M. Hydrochemistry and Carbonate Sediment Characterisation of Bacalar Lagoon, Mexican Caribbean. *Mar. Freshw. Res.* **2019**, *70*, 382. [[CrossRef](#)]
35. Gondwe, B.R.N.; Lerer, S.; Stisen, S.; Marín, L.; Rebolledo-Vieyra, M.; Merediz-Alonso, G.; Bauer-Gottwein, P. Hydrogeology of the South-Eastern Yucatan Peninsula: New Insights from Water Level Measurements, Geochemistry, Geophysics and Remote Sensing. *J. Hydrol.* **2010**, *389*, 1–17. [[CrossRef](#)]
36. Cervantes-Martínez, A.; Mezeta-Barrera, M.; Gutiérrez-Aguirre, M. Basic Limnology of the Karstic Tourist Lake Cenote Azul in Quintana Roo, Mexico. *Hidrobiológica* **2009**, *19*, 177–180.

37. Montes-Ortiz, L.; Elias-Gutierrez, M. Faunistic Survey of the Zooplankton Community in an Oligotrophic Sinkhole, Cenote Azul (Quintana Roo, Mexico), Using Different Sampling Methods, and Documented with DNA Barcodes. *J. Limnol.* **2018**, *77*, 428–440. [[CrossRef](#)]
38. de Jesús-Navarrete, A.; Legorreta, T.Á. Biological Traits Analysis of Free-Living Nematodes as Indicators of Environmental Quality at Lake Bacalar, Mexico. *Limnology* **2022**, *23*, 355–364. [[CrossRef](#)]
39. Castro-Contreras, S.I.; Gingras, M.K.; Pecoits, E.; Aubet, N.R.; Petrash, D.; Castro-Contreras, S.M.; Dick, G.; Planavsky, N.; Konhauser, K.O. Textural and Geochemical Features of Freshwater Microbialites from Laguna Bacalar, Quintana Roo, Mexico. *PALAIOS* **2014**, *29*, 192–209. [[CrossRef](#)]
40. Beltrán Díaz, Y. Estimación de Los Patrones de Fijación de Nitrógeno y Diversidad Asociada (nifH) En Tapices Microbianos y Estromatolitos. Master's Thesis, Universidad Nacional Autónoma de México. Instituto de Ecología, Mexico City, Mexico, 2010.
41. Hernández-Martínez, J.L.; Perera-Burgos, J.A.; Acosta-González, G.; Alvarado-Flores, J.; Li, Y.; Leal-Bautista, R.M. Assessment of Physicochemical Parameters by Remote Sensing of Bacalar Lagoon, Yucatán Peninsula, Mexico. *Water* **2023**, *16*, 159. [[CrossRef](#)]
42. Oliva-Rivera, J.J.; Ocaña, F.A.; De Jesús-Navarrete, A.; De Jesús-Carrillo, R.M.; Vargas-Espósitos, A.A. Reproducción de Pomacea Flagellata (Mollusca: Ampullariidae) En La Laguna de Bacalar, Quintana Roo, México. *Rev. Biol. Trop.* **2016**, *64*, 1643–1650. [[CrossRef](#)] [[PubMed](#)]
43. Mooers, C.N.K.; Maul, G.A. Intra-Americas Sea Circulation. In *Global Coastal Ocean*; Robinson, R., Brink, K.H., Eds.; The Sea; John Wiley & Sons: Hoboken, NJ, USA, 1998; Volume 11, pp. 183–208.
44. Wang, C. Variability of the Caribbean Low-Level Jet and Its Relations to Climate. *Clim. Dyn.* **2007**, *29*, 411–422. [[CrossRef](#)]
45. Rivera-Monroy, V.H.; Farfán, L.M.; Brito-Castillo, L.; Cortés-Ramos, J.; González-Rodríguez, E.; D'Sa, E.J.; Euan-Avila, J.I. Tropical Cyclone Landfall Frequency and Large-Scale Environmental Impacts along Karstic Coastal Regions (Yucatan Peninsula, Mexico). *Appl. Sci.* **2020**, *10*, 5815. [[CrossRef](#)]
46. Mosiño, P.; García, E. The Climate of Mexico. *Climates of North America. World Surv. Climatol.* **1974**, *11*, 345–404.
47. CONAGUA. *Actualización de La Disponibilidad Media Anual de Agua En El Acuífero Península de Yucatán (3105), Estado de Yucatán*; CONAGUA: Ciudad de Mexico, Mexico, 2020.
48. Magaña, V.; Amador, J.A.; Medina, S. The Midsummer Drought over Mexico and Central America. *J. Clim.* **1999**, *12*, 1577–1588. [[CrossRef](#)]
49. Márdero, S.; Nickl, E.; Schmoock, B.; Schneider, L.; Rogan, J.; Christman, Z.; Lawrence, D. Sequías En El Sur de La Península de Yucatán: Análisis de La Variabilidad Anual y Estacional de La Precipitación. *Investig. Geográficas* **2012**, *78*, 19–33. [[CrossRef](#)]
50. Kurczyn, J.A.; Appendini, C.M.; Beier, E.; Sosa-López, A.; López-González, J.; Posada-Vanegas, G. Oceanic and Atmospheric Impact of Central American Cold Surges (Nortes) in the Gulf of Mexico. *Int. J. Climatol.* **2021**, *41*, E1450–E1468. [[CrossRef](#)]
51. Burrough, P.A. *Principles of Geographical Information Systems for Land Resources Assessment. Monographs on Soil and Resources Survey*; Oxford University Press: Oxford, UK, 1986; Volume 12.
52. Wetzel, R.G.; Likens, G.E. *Limnological Analyses*; Springer: New York, NY, USA, 2000; ISBN 978-1-4757-4100-1.
53. Rooy, M. A Rainfall Anomaly Index Independent of Time and Space. *Notos* **1965**, *14*, 43.
54. Wolter, K.; Timlin, M.S. Measuring the Strength of ENSO Events: How Does 1997/98 Rank? *Weather* **1998**, *53*, 315–324. [[CrossRef](#)]
55. Wolter, K.; Timlin, M.S. Monitoring ENSO in COADS with a Seasonally Adjusted Principal Component Index. In *Proceedings of the 17th Climate Diagnostics Workshop*, Norman, OK, USA, 18–23 October 1993; Volume 52.
56. Thomson, R.E.; Emery, W.J. *Data Analysis Methods in Physical Oceanography*; Newnes: Oxford, UK, 2014.
57. Tourian, M.J.; Elmi, O.; Shafaghi, Y.; Behnia, S.; Saemian, P.; Schlesinger, R.; Sneeuw, N. HydroSat: Geometric Quantities of the Global Water Cycle from Geodetic Satellites. *Earth Syst. Sci. Data* **2022**, *14*, 2463–2486. [[CrossRef](#)]
58. Mayer-Gürr, T.; Behzadpur, S.; Ellmer, M.; Kvas, A.; Klinger, B.; Strasser, S.; Zehentner, N. ITSG-Grace2018-Monthly, Daily and Static Gravity Field Solutions from GRACE. Data set/Database. 2018. [[CrossRef](#)]
59. Kvas, A.; Behzadpour, S.; Ellmer, M.; Klinger, B.; Strasser, S.; Zehentner, N.; Mayer-Gürr, T. ITSG-Grace2018: Overview and Evaluation of a New GRACE-Only Gravity Field Time Series. *J. Geophys. Res. Solid Earth* **2019**, *124*, 9332–9344. [[CrossRef](#)]
60. Klees, R.; Zapreeva, E.; Winsemius, H.; Savenije, H. The Bias in GRACE Estimates of Continental Water Storage Variations. *Hydrol. Earth Syst. Sci.* **2007**, *11*, 1227–1241. [[CrossRef](#)]
61. Seekell, D.A.; Byström, P.; Karlsson, J. Lake Morphometry Moderates the Relationship between Water Color and Fish Biomass in Small Boreal Lakes. *Limnol. Oceanogr.* **2018**, *63*, 2171–2178. [[CrossRef](#)]
62. Kebedew, M.G.; Kibret, A.A.; Tilahun, S.A.; Belete, M.A.; Zimale, F.A.; Steenhuis, T.S. The Relationship of Lake Morphometry and Phosphorus Dynamics of a Tropical Highland Lake: Lake Tana, Ethiopia. *Water* **2020**, *12*, 2243. [[CrossRef](#)]
63. Carrillo, L.; Palacios-Hernández, E.; Yescas, M.; Ramírez-Manguilar, A.M. Spatial and Seasonal Patterns of Salinity in a Large and Shallow Tropical Estuary of the Western Caribbean. *Estuaries Coasts* **2009**, *32*, 906–916. [[CrossRef](#)]
64. Alcérreca-Huerta, J.C.; Álvarez-Legorreta, T.; Carrillo, L.; Flórez-Franco, L.M.; Reyes-Mendoza, O.F.; Sánchez-Sánchez, J.A. First Insights into an Exceptionally Deep Blue Hole in the Western Caribbean: The Taam Ja'Blue Hole. *Front. Mar. Sci.* **2023**, *10*, 346. [[CrossRef](#)]
65. Pope, K.O.; Ocampo, A.C.; Fischer, A.G.; Vega, F.J.; Ames, D.E.; King Jr, D.T.; Fouke, B.W.; Wachtman, R.J.; Kletetschka, G. Chicxulub Impact Ejecta Deposits in Southern Quintana Roo, México, and Central Belize. *Geol. Soc. Am. Spec. Pap.* **2005**, *384*, 171–190.

66. Perry, E.C.; Leal-Bautista, R.M.; Velázquez-Olimán, G.; Sánchez-Sánchez, J.A.; Wagner, N. Aspects of the Hydrogeology of Southern Campeche and Quintana Roo, Mexico. *Bol. Soc. Geológica Mex.* **2021**, *73*, A011020. [CrossRef]
67. Zhao, Z.; Han, M.; Yang, K.; Holbrook, N.J. Signatures of Midsummer Droughts over Central America and Mexico. *Clim. Dyn.* **2022**, *60*, 3523–3542. [CrossRef]
68. CONAGUA. *Estado Del Clima En México Durante 2020 y Perspectivas Para 2021*; CONAGUA: Ciudad de Mexico, Mexico, 2021.
69. Talling, J. Environmental Controls on the Functioning of Shallow Tropical Lakes. *Hydrobiologia* **2001**, *458*, 1–8. [CrossRef]
70. Bhatia, R.; Jain, D. Water Quality Assessment of Lake Water: A Review. *Sustain. Water Resour. Manag.* **2016**, *2*, 161–173. [CrossRef]
71. Hernández-Cerda, M.E.; Azpra Romero, E.; Lomas Barrié, C.T. Cristóbal, the Tropical Storm in 2020 That Left Atypical Rainfall in the Yucatan Peninsula. *Entorno Geográfico* **2021**, 125–156. [CrossRef]
72. Castro-Chan, R.A.; De Jesús Navarrete, A.; Zavala Mendoza, A. *Estudio Para Establecer Las Causas de La Mortalidad Masiva Del Caracol de Agua Dulce Chivita Pomacea Flagellata*; Consejo Quintanarroense de Ciencia y Tecnología: Chetumal, Mexico, 2021.
73. Álvarez-Legorreta, T.; Carrillo-Bibriezca, L.; De Jesús Navarrete, A.; Herrera-Silveira, J.; Gutiérrez, M.; Cervantes, A. *Desarrollo de Indicadores de Calidad Del Agua En Lagunas Costeras y Continentales de Quintana Roo Para El Diseño e Implementación de Un Programa de Monitoreo Estatal*; FOMIX: Chetumal, Quintana Roo, Mexico, 2011; p. 174.
74. Álvarez-Legorreta, T. ¿La calidad del agua de Laguna Bacalar ha cambiado? In: Foro 2020 Agua Clara Bacalar. Situación Actual de la Laguna de Bacalar. Agua Clara: Bacalar, Mexico. 2020. Available online: https://www.youtube.com/watch?v=7nqy_lei-xI (accessed on 13 February 2023).
75. CONAGUA. *Reseña Del Huracán “Dean” Del Océano Atlántico*; CONAGUA: Ciudad de Mexico, Mexico, 2007.
76. Islebe, G.; Torrescano-Valle, N.; Valdéz-Hernández, M.; Tuz-Novelo, M.; Weissenberger, H. Efectos Del Impacto Del Huracán Dean En La Vegetación Del Sureste de Quintana Roo, México. *For. Veracruzana* **2009**, *11*, 1–6.
77. Ramírez-Barajas, P.J.; Islebe, G.; Torrescano-Valle, N. Post-Hurricane Dean Impact on Habitat and Its Influence on the Relative Abundance of Large Vertebrates in the Selva Maya, Quintana Roo, Mexico. *Rev. Mex. Biodivers.* **2012**, *83*, 1194–1207.
78. CONAGUA. *Reseña Del Huracán Karl Del Océano Atlántico*; CONAGUA: Ciudad de Mexico, Mexico, 2010.
79. Perry, E.; Paytan, A.; Pedersen, B.; Velazquez-Oliman, G. Groundwater Geochemistry of the Yucatan Peninsula, Mexico: Constraints on Stratigraphy and Hydrogeology. *J. Hydrol.* **2009**, *367*, 27–40. [CrossRef]
80. Perry, E.C.; Velazquez-Oliman, G.; Leal-Bautista, R.M.; Dunning, N.P. The Icaiche Formation: Major Contributor to the Stratigraphy, Hydrogeochemistry and Geomorphology of the Northern Yucatán Peninsula, Mexico. *Bol. Soc. Geológica Mex.* **2019**, *71*, 741–760. [CrossRef]
81. CONAGUA. *Se Mantiene en Vigilancia el Nivel del Río Champotón en Campeche*; CONAGUA: Ciudad de Mexico, Mexico, 2020; p. 1.
82. SEDETUR. Indicadores Turísticos. Available online: <https://qroo.gob.mx/sedetur/indicadores-turisticos> (accessed on 6 January 2022).
83. Rojas-Castillo, L.A.; Calderón-Maya, J.R. Etapas Del Proceso de Urbanización En La Ciudad de Bacalar, Quintana Roo (México). *Quivera Rev. Estud. Territ.* **2022**, *25*, 5–19. [CrossRef]
84. Gómez-García, M. Evaluación Del Cambio de Uso de Suelo Ocasionado Por Actividades Antrópicas En El Área Del Programa de Ordenamiento Ecológico Territorial de Bacalar, Quintana Roo. Bachelor’s Thesis, Universidad Nacional Autónoma de México, Mexico City, Mexico, 2018.
85. INEGI. Censo de población y vivienda 2020. Available online: <https://www.inegi.org.mx/programas/ccpv/2020/default.html> (accessed on 31 May 2022).
86. Huchin-Ochoa, S.A.; Navarro-Martínez, A.; Ellis, E.A.; Hernández Gómez, I.U. Deforestación En El Municipio de Bacalar, Quintana Roo, México Durante El Período 1993–2017. *Madera Bosques* **2022**, *28*, e2832396. [CrossRef]
87. Ellis, E.A.; Navarro Martínez, A.; García Ortega, M.; Hernández Gómez, I.U.; Castillo, D.C. Forest Cover Dynamics in the Selva Maya of Central and Southern Quintana Roo, Mexico: Deforestation or Degradation? *J. Land Use Sci.* **2020**, *15*, 25–51. [CrossRef]
88. Gómez-Pech, E.H.; Barrasa García, S.; García de Fuentes, A. Paisaje Litoral de La Laguna de Bacalar (Quintana Roo, México): Ocupación Del Suelo y Producción Del Imaginario Por El Turismo. *Investig. Geográficas* **2018**. [CrossRef]
89. Smith, D.N.; Ortega-Camacho, D.; Acosta-González, G.; Leal-Bautista, R.M.; Fox, W.E.; Cejudo, E. A Multi-Approach Assessment of Land Use Effects on Groundwater Quality in a Karstic Aquifer. *Heliyon* **2020**, *6*, e03970. [CrossRef] [PubMed]
90. UNESCO. *UN-Water United Nations World Water Development Report 2020: Water and Climate Change*; UNESCO: Paris, France, 2020.

Disclaimer/Publisher’s Note: The statements, opinions and data contained in all publications are solely those of the individual author(s) and contributor(s) and not of MDPI and/or the editor(s). MDPI and/or the editor(s) disclaim responsibility for any injury to people or property resulting from any ideas, methods, instructions or products referred to in the content.